Long-ranged contributions to solvation free energies from theory and short-ranged models

Richard C. Remsing[a,b], Shule Liu[c,d], and John D. Weeks[a,c,1]

[a]Institute for Physical Science and Technology and Chemical Physics Program, University of Maryland, College Park, MD 20742; [b]Institute for Computational Molecular Science, Temple University, Philadelphia, PA 19122; [c]Department of Chemistry and Biochemistry, University of Maryland, College Park, MD 20742; and [d]Department of Chemistry, James Franck Institute and Computation Institute, University of Chicago, Chicago, IL 60637

This contribution is part of the special series of Inaugural Articles by members of the National Academy of Sciences elected in 2009.

Contributed by John D. Weeks, January 13, 2016 (sent for review November 2, 2015; reviewed by Gerhard Hummer, Roland R. Netz, and Frank H. Stillinger)

Long-standing problems associated with long-ranged electrostatic interactions have plagued theory and simulation alike. Traditional lattice sum (Ewald-like) treatments of Coulomb interactions add significant overhead to computer simulations and can produce artifacts from spurious interactions between simulation cell images. These subtle issues become particularly apparent when estimating thermodynamic quantities, such as free energies of solvation in charged and polar systems, to which long-ranged Coulomb interactions typically make a large contribution. In this paper, we develop a framework for determining very accurate solvation free energies of systems with long-ranged interactions from models that interact with purely short-ranged potentials. Our approach is generally applicable and can be combined with existing computational and theoretical techniques for estimating solvation thermodynamics. We demonstrate the utility of our approach by examining the hydration thermodynamics of hydrophobic and ionic solutes and the solvation of a large, highly charged colloid that exhibits overcharging, a complex nonlinear electrostatic phenomenon whereby counterions from the solvent effectively overscreen and locally invert the integrated charge of the solvated object.

mean field theory | free energy calculations | density functional theory | hydrophobicity | solvation

Solvation thermodynamics underlies a vast array of important processes, ranging from protein folding (1, 2) and ligand binding (3) to self-assembly at interfaces (4). Thus, understanding solvation, and driving forces rooted in solvation, has been a focus of chemistry and physics for over a century (5, 6).

Quantitatively successful theories of self-solvation and solvophobic solvation in simple fluids have been developed (7–16). However, a generally useful analytic approach for solvation in complex charged and polar environments is lacking, and solvation is typically studied with computer simulations. Contributions from the long-ranged components of Coulomb interactions in periodic images of the simulation cell are typically evaluated using computationally intense Ewald and related lattice summation techniques (17). These methods generate distorted, system size-dependent interaction potentials (18) and do not scale well in massively parallel simulations (19), adding considerable computational overhead. Moreover, artifacts can arise from spurious interactions between the periodic images of solutes, as observed for proteins in water (20).

The local molecular field (LMF) theory of nonuniform fluids is a promising avenue for substantially improving free energy calculations by removing many of the computational and conceptual burdens associated with long-ranged interactions (14, 21). LMF theory prescribes a way to accurately determine the structure of a full system with long-ranged intermolecular interactions in a general single particle field by studying a simpler mimic system wherein particles interact with short-ranged intermolecular interactions only. An effective field in the mimic system accounts for the averaged effects of the long-ranged "far-field" interactions in the full system.

This approach is especially powerful for studying solvation in charged and polar solvents, where in the simplest case the effective field can represent the interactions between a fixed solute and the solvent. In this paper, we show that when the effective field and induced density around the solute are accurately determined by LMF theory it is very easy to integrate over the solvent structure and accurately compute the far-field contributions to the solvation free energy as well, using quantities determined solely in the short-ranged mimic system, where simulations scale linearly with system size.

LMF theory presents a general conceptual framework that gives qualitative as well as quantitative insight into many other problems. Its treatment of long- and short-ranged forces makes suggestive connections to other well-established theoretical methods, such as perturbation theory for uniform simple fluids (6, 7), classical density functional theory (DFT) of nonuniform fluids (11), and the successful quasichemical approach for solvation (16). Although our focus in this paper is on the quantitative determination of the solvation free energy, many of these connections will be touched upon in our discussion here and in *Supporting Information*. The treatment of solvation free energies we present here can be readily generalized to determine more complex free energies, including alchemical transformations and potentials of mean force (3), and extended to more general charged and polar mixtures (21) with mobile solutes.

The conceptual development of the LMF approach to solvation thermodynamics is introduced in the next section, with derivations

Significance

Many important biological and industrial processes, ranging from protein folding and ligand binding to self-assembly of materials at interfaces, take place in solution and are mediated by driving forces rooted in solvation. However, conceptual and computational difficulties arising from long-ranged Coulomb interactions still present a challenge to current approaches. Here we present a framework to determine very accurately the long-ranged contributions to solvation free energies in charged and polar systems from models with only short-ranged, local interactions. We examine a variety of ubiquitous solvation processes, including hydrophobic and ionic hydration, as well as colloidal overcharging. The theory additionally suggests ways to improve density functional theories of solvation by providing insights into commonly used approximations.

Author contributions: R.C.R., S.L., and J.D.W. designed research; R.C.R., S.L., and J.D.W. performed research; R.C.R., S.L., and J.D.W. analyzed data; and R.C.R. and J.D.W. wrote the paper.

Reviewers: G.H., Max Planck Institute of Biophysics; R.R.N., Free University of Berlin; and F.H.S., Princeton University.

The authors declare no conflict of interest.

[1]To whom correspondence should be addressed. Email: jdw@umd.edu.

This article contains supporting information online at www.pnas.org/lookup/suppl/doi:10.1073/pnas.1521570113/-/DCSupplemental.

and other technical details given in *Materials and Methods*, *Derivation of the Far-Field Solvation Free Energy* and *Supporting Information*. We first focus on the solvophobic solvation of a repulsive, spherical solute in a Lennard-Jones (LJ) fluid, where most of the ideas can be understood in their simplest form and the basic physics is well understood. We then turn to more challenging and experimentally relevant problems involving the length-scale transition in hydrophobic solvation of an apolar solute in water and its effect on the solvation free energies; the hydration of single ions is discussed in *Supporting Information*. Finally we discuss the solvation and "overcharging" of a large, highly charged colloid in an ionic fluid, a highly nontrivial process involving ion correlations (22) that is completely missed in classic mean field treatments of ionic solutions (23).

LMF Theory and Truncated Models

For simplicity, we first study solvation in a one-component LJ fluid with pairwise intermolecular interactions. We assume that the intermolecular interactions in the full solvent system are slowly varying at large separations, as is true for both LJ and Coulomb interactions. In the simplest description of solvation using the Grand ensemble, the solvent interacts with an external field $\phi(\mathbf{r})$ from a fixed solute. This induces a nonuniform density $\rho(\mathbf{r})$ that far from the solute or when $\phi \to 0$ reduces to the known bulk density ρ_B associated with a chemical potential μ.

In a general perturbation approach (6, 7), the intermolecular interactions of both solute and solvent are usually divided into strong short-ranged reference and slowly varying long-ranged perturbation parts (14):

$$u(r) = u_0(r) + u_1(r), \qquad [1]$$

$$\phi(\mathbf{r}) = \phi_0(\mathbf{r}) + \phi_1(\mathbf{r}). \qquad [2]$$

The simplest "strong coupling" (SC) reference system, denoted by a subscript 0, ignores all effects of the long-ranged $u_1(r)$ and has short-ranged pair interactions $u_0(r)$ along with a similarly chosen short-ranged solute–solvent field $\phi_0(\mathbf{r})$ (21). In general the induced density $\rho_0(\mathbf{r})$ in the SC reference system will differ from the $\rho(\mathbf{r})$ of the full system but the chemical potential μ_0 is chosen so that the density again approaches ρ_B far from the solute.

LMF theory considers a special reference system or "mimic system," denoted by the subscript R, resulting from a judicious choice of the short- and long-ranged components of $u(r)$ along with an effective or renormalized solute field $\phi_R(\mathbf{r})$, chosen in principle such that the induced density in the mimic system equals that of the full system:

$$\rho_R(\mathbf{r};[\phi_R]) = \rho(\mathbf{r};[\phi]). \qquad [3]$$

Here we have explicitly indicated the functional dependence of the densities on their respective fields. This dependence will be omitted in what follows unless needed for clarity.

As discussed in detail in ref. 21 and further in *Supporting Information*, extensive previous work has shown that $\phi_R(\mathbf{r})$ and $\rho_R(\mathbf{r})$ can often be very accurately determined by solving the LMF equation,

$$\phi_R(\mathbf{r}) = \phi(\mathbf{r}) + \int d\mathbf{r}' [\rho_R(\mathbf{r}') - \rho_B] u_1(|\mathbf{r} - \mathbf{r}'|). \qquad [4]$$

Here constants have been chosen so that ϕ_R vanishes in the bulk or when ϕ is zero. This equation also holds in other ensembles such as the constant-pressure ensemble where the density exactly approaches ρ_B far from the solute.

The LMF equation has a functional form suggested by a simple mean field approximation where the averaged effects of the long-ranged intermolecular pair interactions are self-consistently related to the density induced by a single particle mean field. However, this form is derived by an approximate integration over intermolecular forces in the full and mimic systems as described by the exact Yvon–Born–Green (YBG) hierarchy of equations (14, 21) and does not use the traditional mean field ansatz where pair distribution functions are approximated by products of single particle functions. The detailed analysis in ref. 21 and *Supporting Information* shows that quantitatively accurate results from the LMF equation can be expected only when the $u_1(r)$ component averaged over is uniformly slowly varying, as illustrated in the Weeks–Chandler–Andersen (WCA) separation of the LJ potential (7, 14). This requirement will be especially important in the derivation of the solvation free energy, as discussed in the next section.

LMF theory can be immediately adapted to models of charged and polar systems with pairwise Coulomb interactions (21). Experience has shown that it is advantageous to separate the Coulomb interaction from all charges into short- and long-ranged parts according to

$$\frac{1}{r} \equiv v(r) = \frac{\mathrm{erfc}(r/\sigma)}{r} + \frac{\mathrm{erf}(r/\sigma)}{r} \equiv v_0(r) + v_1(r), \qquad [5]$$

where $\mathrm{erf}(r)$ and $\mathrm{erfc}(r) = 1 - \mathrm{erf}(r)$ are the usual error and complementary error functions. $v_1(r)$ is the electrostatic potential (given by a convolution with $1/r$) arising from a unit Gaussian charge distribution

$$\rho_G(\mathbf{r}) = \frac{1}{\pi^{3/2}\sigma^3} \exp\left(-\frac{r^2}{\sigma^2}\right). \qquad [6]$$

For accurate results from LMF theory the smoothing length σ should generally be chosen on the order of typical nearest-neighbor distances. The Coulomb LMF equation analogous to Eq. **4** can be written as (21)

$$\mathcal{V}_R(\mathbf{r}) = \mathcal{V}(\mathbf{r}) + \int d\mathbf{r}' \rho_R^q(\mathbf{r}') v_1(|\mathbf{r} - \mathbf{r}'|) \qquad [7]$$

$$= \mathcal{V}(\mathbf{r}) + \int d\mathbf{r}' \, \rho_R^{q\sigma}(\mathbf{r}') \cdot \frac{1}{|\mathbf{r} - \mathbf{r}'|}. \qquad [8]$$

Here $\mathcal{V}(\mathbf{r})$ is the bare electrostatic potential from the solute and $\rho_R^q(\mathbf{r})$ is the equilibrium charge density of the mobile solvent where $\rho_B^q = 0$. In Eq. **8** we have used the convolution form of v_1 to rewrite the renormalized potential in terms of the Gaussian smoothed charged density $\rho_R^{q\sigma}$, the convolution of $\rho_R^q(\mathbf{r})$ with ρ_G. As shown below, $\rho_R^{q\sigma}$ plays a fundamental role in solvation processes in charged and polar systems (21). Hu (24) has shown that a similar Gaussian smoothing of the instantaneous charge density in each configuration permits the efficient determination of certain dynamical properties in cases of high symmetry.

LMF Thermodynamic Cycle for Solvation

We first consider the solvation of a rigid solute (S) fixed at the origin in a mobile single-component LJ-type solvent (M). Fig. 1 schematically depicts the process of gradually "turning on" the solute–solvent interaction potential $\phi(\mathbf{r})$. This is harshly repulsive at short distances where molecular cores between the solute and solvent will overlap, and more generally may also contain other strong short-ranged forces describing hydrogen bonding and other local interactions as well as long-ranged interactions. We want to determine the solvation free energy $\tilde{\Omega}[\phi] \equiv \Omega[\phi] - \Omega[\phi = 0]$, the difference in the Grand free energy between the full solvent–solute system and the pure solvent in zero solute field.

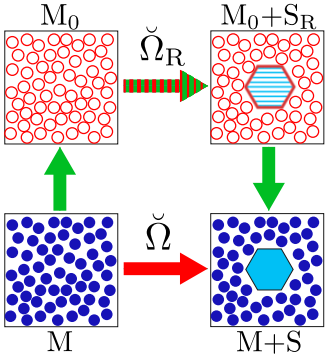

Fig. 1. LMF theory-based thermodynamic cycle for solvation. The bottom leg of the cycle corresponds to inserting a solute (S) into a mobile solvent (M), both of which have short- and long-ranged interactions. This solvation process results in a free energy change $\breve{\Omega}$. The top leg of the cycle depicts the insertion of a renormalized solute (S_R) into a short-ranged mobile solvent (M_0), and the solvation free energy in this mimic system is $\breve{\Omega}$. The sum of the free energies of the paths depicted by green arrows is $\Delta\Omega_{LMF} = \breve{\Omega} - \breve{\Omega}_R$, as described in the text.

The lower left panel of Fig. 1 shows the core positions of the mobile bulk solvent (M) in a typical configuration. The solvent molecules interact with the full long-ranged pair potential u. The lower right panel schematically depicts an equilibrium configuration of the full solute–solvent system, where the solute (S) has been inserted into the fluid.

However, the transformation from a noninteracting point solute on the left into the full solute on the right must generally be carried out in small steps using a series of nonphysical intermediate states as the harshly repulsive solute–solvent core interactions are gradually turned on (3). Moreover, each step of this process requires an accurate treatment of the long-ranged interactions, which for Coulomb interactions adds significant overhead to each time step. We indicate this general difficulty by using a red arrow to connect the two lower panels of Fig. 1.

The LMF treatment of solvation in Fig. 1 introduces a thermodynamic cycle involving a short-ranged mimic system that eliminates most of the problems arising from conventional treatments of long-ranged forces. Moreover, it provides a natural and physically suggestive way of partitioning the free energy into short and long-ranged components that are conceptually related to elements of the quasichemical theory of solvation (16, 25). These connections will be discussed in detail in a future publication; here we focus on the important far-field contribution to the solvation free energy, which plays a fundamental role in all partitioning schemes.

The LMF thermodynamic cycle includes the two upper panels of Fig. 1, which describe solvation in the short-ranged mimic system. The upper left panel illustrates a configuration of the strong coupling or mimic solvent (M_0); the red color indicates truncated solvent–solvent interactions, $u_0(r)$. The slowly varying, long-ranged components of the intermolecular forces tend to cancel in a uniform fluid (6, 7) so the particle arrangements are similar in the bulk M and M_0 panels.

Solvation in the mimic system involves insertion of a mimic solute (S_R), described by the renormalized potential

$$\phi_R(\mathbf{r}) \equiv \phi_0(\mathbf{r}) + \phi_{R1}(\mathbf{r}). \quad [9]$$

The slowly varying component $\phi_{R1}(\mathbf{r})$ is given by the sum of the slowly varying $\phi_1(\mathbf{r})$ part of the solute–solvent interaction in Eq. **2** and the last term on the right in the LMF Eq. **4**. This latter term is also slowly varying because of the integration over u_1. As prescribed by LMF theory, $\phi_R(\mathbf{r})$ is chosen so that the induced density around the mimic solute in the right $M_0 + S_R$ panel is very similar to that around the full solute in the M + S panel, as indicated in Fig. 1.

We exploit this fact in determining the far-field component of the solvation free energy: the free energy change between the lower and upper panels on the left and right sides of Fig. 1, indicated by the vertical green arrows. By a "bottom-up" functional integration over the effective field and induced density as connected by the LMF equation and paying close attention to constant terms, we derive in *Materials and Methods*, *Derivation of the Far-Field Solvation Free Energy* a simple, analytic expression for the far-field component of the solvation free energy

$$\Delta\Omega_{LMF}[\phi_R] \equiv \breve{\Omega}[\phi] - \breve{\Omega}_R[\phi_R] \quad [10]$$

$$= -\frac{1}{2}\int d\mathbf{r}\,[\rho(\mathbf{r}) + \rho_B][\phi_R(\mathbf{r}) - \phi(\mathbf{r})]. \quad [11]$$

Eq. **11** is our main result. It can be immediately generalized as in Eq. **7** for charged and polar systems as

$$\Delta\Omega_{LMF}[\mathcal{V}_R] = -\frac{1}{2}\int d\mathbf{r}\rho_R^q(\mathbf{r})[\mathcal{V}_R(\mathbf{r}) - \mathcal{V}(\mathbf{r})] \quad [12]$$

and extended to describe free energies as a function of a general order parameter, suggesting that this LMF-based framework is widely applicable.

The validity of Eq. **11** relies on the mean field form and accuracy of the LMF Eq. **4**, which can generally be justified only for particular slowly varying choices of the u_1 term. This important constraint is completely missed in conventional "top-down" DFT approaches where a crude and uncontrolled mean field product approximation is usually imposed directly on pair correlations in the free energy functional itself. See *Materials and Methods*, *Derivation of the Far-Field Solvation Free Energy* and *Supporting Information* for further discussion of this important conceptual point.

To complete the cycle we must calculate the solvation free energy in the short-ranged mimic system, $\breve{\Omega}_R$. It can be determined using standard methods where the $\phi_R(\mathbf{r})$ interaction is gradually turned on. Because $\phi_R(\mathbf{r})$ contains all of the strong short-ranged interactions $\phi_0(\mathbf{r})$, this process is inherently difficult and typically would require just as many intermediate steps as the analogous solvation process in the full system. However, each step can be carried out much more efficiently in the absence of long-ranged interactions. This major simplification is suggested by green stripes on the arrow connecting the upper panels in Fig. 1 and contrasts with the red arrow connecting the lower panels.

Moreover, Eq. **9** allows us to write $\breve{\Omega}_R$ as the sum of $\breve{\Omega}_0[\phi_0]$, the solvation free energy in the short-ranged SC system with the known field $\phi_0(\mathbf{r})$, and the additional free energy, $\Delta\Omega_{R1}$, of turning on the more slowly varying $\phi_{R1}(\mathbf{r})$. The latter can often be determined in a numerically practical and computationally efficient way that requires no simulations of the mimic system by using linear response theory to reweight configurations in the SC system, as shown in ref. 26. When linear response is accurate it can be numerically useful to remove cancelling terms by combining $\Delta\Omega_{R1}$ with $\Delta\Omega_{LMF}$, as discussed in *Supporting Information*.

Length Scale Dependence of Solvophobic Solvation

The crux of the LMF treatment of solvation is that accurate thermodynamic properties follow immediately from a good description of the induced solvent structure. To illustrate this point, we first show that LMF theory can quantitatively capture the drying in an LJ fluid observed at the surface of a harshly repulsive solute with an effective hard sphere diameter $R_{HS} \approx 2\sigma_{LJ}$, as defined in ref. 27.

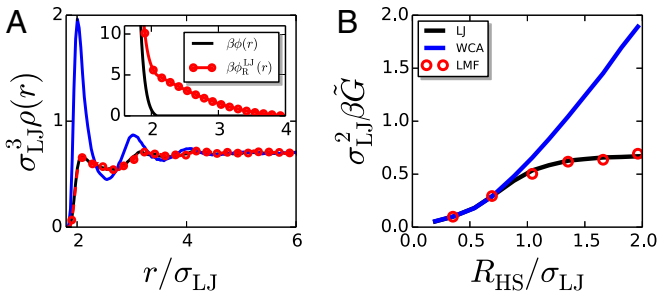

Fig. 2. (*A*) Nonuniform density around a repulsive sphere of radius $R_{HS} \approx 2\sigma_{LJ}$ in an LJ fluid and in its corresponding WCA reference system and LMF theory mimic system. (*Inset*) The bare and renormalized solute fields, $\phi(r)$ and $\phi_R(r)$, respectively. (*B*) Solvation free energies as a function of solute radius in LJ and WCA fluids scaled by the solute surface area, $\tilde{G} = \bar{G}/4\pi R_{HS}^2$.

As illustrated in Fig. 2*A*, the WCA solvent strongly wets the solute surface at large $R_{HS} \approx 2\sigma_{LJ}$. Nevertheless, drying can be obtained with a WCA solvent by using LMF theory to account for the averaged effects of unbalanced LJ forces at the fluid–solute interface. The renormalized solute potential $\phi_R(\mathbf{r})$, is compared with the bare potential $\phi(\mathbf{r})$ in Fig. 2*A*, *Inset*. The field $\phi_R(r)$ provides an effective "push" on solvent particles near the interface, such that the density in the mimic system is nearly identical to that in the full LJ system.

Given this accurate description of structure from LMF theory, we now study the solvation thermodynamics of harshly repulsive spherical solutes of various sizes in LJ and WCA fluids. Detailed simulation results are shown in Fig. 2*B*. The Gibbs free energies of solvation, $\bar{G}$, for the repulsive solutes in the WCA system scale with solute volume for all sizes, whereas solvation in the full LJ system displays a cross-over from scaling with solute volume to solute surface area at $R_{HS} \approx \sigma_{LJ}$, consistent with the appearance of interfacial drying (13, 14, 27, 28). The LMF prediction from Eq. **11** is then used to obtain the far-field correction to the WCA solvation free energies. The LMF free energies recover the length-scale transition and reproduce the LJ solvation free energies with quantitative accuracy.

The computational utility of LMF theory becomes more apparent in systems with costly long-ranged electrostatic interactions. We first illustrate this by studying hydrophobic solvation of repulsive spheres in water, in complete analogy to solvophobic solvation in LJ fluids. In the short-ranged SC reference system, extended simple point charge (SPC/E) water is modeled in a Gaussian-truncated (GT) fashion, wherein the $1/r$ portion of the Coulomb potential is replaced by the short-ranged $v_0(r)$. The smoothing length $\sigma = 4.5$ Å is chosen such that $v_0(r)$ captures the strong, local interactions leading to H-bonding, so that the resulting GT water model accurately reproduces the molecular structure and local properties of the H-bond network of bulk water (27, 28). Because the H-bond network of water is maintained around small solutes (27–29), GT water also provides a very good description of solvation free energies in the small solute regime (27) (Fig. 3*D*).

Drying at the surface of a large repulsive sphere associated with breaking local hydrogen bonds should also be qualitatively captured by GT water, as shown in Fig. 3*A*. However, small differences in the nonuniform water density $\rho(r)$ can be seen. These arise because the long-ranged electrostatics generates subtle long wavelength perturbations of the local hydrogen bond network around the solute to produce dielectric screening and related effects (30–32).

These differences are most clearly seen in the Gaussian smoothed charge density, $\rho^{q\sigma}(\mathbf{r})$, appearing in the LMF Eq. **8**. Smoothed charge densities for GT and full water are shown in Fig. 3*B*. Water is polarized at the solute interface even in the full system, evidenced by the positive lobe in $\rho^{q\sigma}(r)$ at small r. This buildup of polarization is effectively screened, consistent with the subsequent negative peak and $\rho^{q\sigma}(r) \to 0$ for large r. In GT water, however, only local hydrogen bonding constraints are optimized and a much larger positive peak at small r is observed, indicating overpolarization at the solute surface. Moreover, this peak is largely unscreened; only a small peak develops at large r, and $\rho^{q\sigma}(r)$ does not reach zero until the end of the (neutral) simulation box.

The picture provided by $\rho^{q\sigma}(\mathbf{r})$ is complemented by examining the orientational structure of hydration shell water in atomistic detail. The probability distribution, $P(\theta_{OH})$, of the angle, θ_{OH}, made by the O–H bond of water and the distance vector connecting the water oxygen and the solute center, shown in Fig. 3*C*, further illustrates that long-ranged electrostatics—mainly dipole-dipole interactions in the case of water—significantly influences the polarization of interfacial water. GT water overorients its O–H bonds toward the solute with respect to the full water model, because the drive to form a dangling O–H bond at a nonpolar interface arises from local, short-ranged interactions (9, 27). The dipolar screening in full water reduces this tendency to form dangling bonds.

We can now integrate over structure and obtain the LMF contribution to the solvation free energy as in Eq. **12**. Owing to the similar local structure of the full and GT water systems, accurate estimates of $\rho_R^q(r)$, and therefore $\mathcal{V}_{R1}(r)$, can be obtained from simulations in the GT system alone by using the linear response theory formalism of Hu and Weeks (26); in fact, this simplification holds for almost all charged and polar systems we have examined (see *Supporting Information* for more details). The electrostatic LMF correction determined in this manner brings the hydration free energies into quantitative agreement with those of the full system, as shown in Fig. 3*D*.

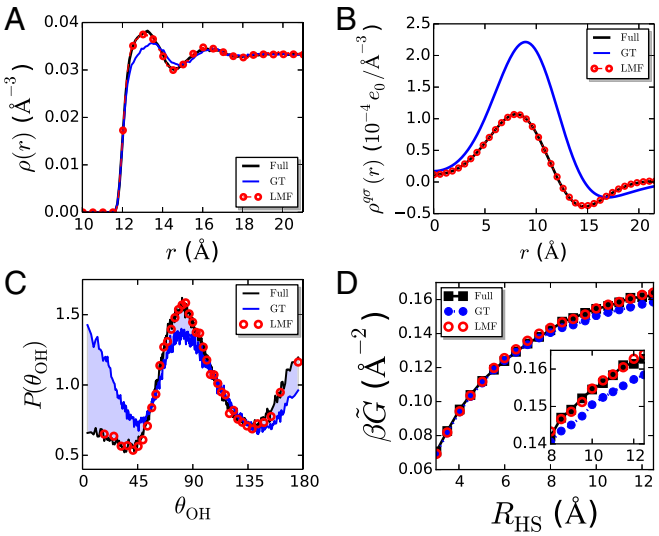

Fig. 3. (*A*) The nonuniform density $\rho(r)$ and (*B*) the Gaussian smoothed charge density $\rho^{q\sigma}(r)$ of water around a harshly repulsive solute with an effective hard sphere diameter of $R_{HS} \approx 12$ Å for the full SPC/E, GT, and LMF theory mimic systems. Note that the Gaussian smoothing results in nonzero $\rho^{q\sigma}(r)$ inside the solute core. (*C*) The probability distribution, $P(\theta_{OH})$, of the angle made by water O–H bonds and the water–solute distance vector for the same systems. The shaded region serves to highlight the deviation of the GT system from the full results. (*D*) Solvation free energies scaled by the solute surface area, $\tilde{G} = \bar{G}/4\pi R_{HS}^2$, obtained in the full, GT, and LMF systems. (*Inset*) The behavior of the free energies at large R_{HS}. LMF corrections are on the order of 10 k_BT at $R_{HS} = 12$ Å.

Solvation and Overcharging in Colloidal Systems

We now turn to a case where long-ranged electrostatic interactions play a major role in determining both the structure and thermodynamics of the system, solvation of a charged colloid in an ionic fluid. Large, highly charged colloidal particles can seemingly invert their charge when immersed in solutions of multivalent counterions (23). Multivalent counterions adsorb to the surface of the colloid at densities high enough that the net charge contained inside the first solvation shell is opposite to that of the colloid. This phenomenon, known as overcharging, is highly nontrivial (22) and cannot be captured by classic mean field theories of ionic solutions (23).

Here we consider the solvation of a large ($R_C = 30$ Å), highly charged ($Q_C = -110e_0$) colloid in a system of trivalent counterions and monovalent coions in implicit water with a uniform dielectric constant ε as modeled in ref. 33. The charge is uniformly smeared over the colloid surface, and the colloid and counterions are modeled as charged WCA species (7). The SC system is constructed with a smoothing length of $\sigma = 2.5a = 26.828$ Å, where a is the nearest-neighbor distance defined setting $4\pi a^3(\rho^+ + \rho^-)/3$ equal to unity and $\rho^{\pm}$ is the density of counter (+) or co(−) ions.

As a measure of the solvation structure, we monitor the integrated charge,

$$Q(r) = Q_C + \int_0^r dr' 4\pi r'^2 \rho^q(r'), \qquad [13]$$

shown in Fig. 4*A*. This quantity describes how the solute charge is screened by the solvent charges. We find overcharging of the colloid by the ionic solvent, with a maximum inverted charge of $0.15Q_C \approx 16.5e_0$ near the solute surface.

Overcharging in the SC system is substantially less than that in the full system, indicating that long-ranged electrostatics plays an important role in determining the colloid solvation structure. Additionally, the SC system does not capture the local neutrality of the system, because its $Q(r)$ reaches zero only when integrating over the entire box. In contrast, the full system $Q(r)$ approaches zero at a distance about twice the radius of the colloid, indicating that the solute charge is completely screened over this length scale. The LMF potential provides the renormalized force necessary to quantitatively describe the amount of overcharging and the screening length in this complex system, as evidenced by the $Q(r)$ in Fig. 4*A*.

These large corrections to the SC system suggest that long-ranged interactions will make a significant contribution to the colloidal solvation free energy $\beta G \equiv \beta G_R + \beta\Delta G_{LMF}$ as well. Indeed, the far-field LMF term, $\beta\Delta G_{LMF} = -1{,}049$, whereas $\beta G_R = -244$. The LMF result $\beta G = -1{,}293$ is in very good agreement with that determined using conventional techniques (33), $\beta G_{Ewald} = -1{,}294$.

We also obtained the free energy of charging the colloid to intermediate charges (Q) between 0 and Q_C. This $G(Q)$ scales quadratically with Q to a good approximation, as shown in Fig. 4*B*, *Inset*. The charge dependence is dominated by the LMF contribution, which itself is quadratic in Q.

The quadratic dependence of ΔG_{LMF} on Q can be rationalized by noting that the long-ranged electrostatic behavior is very insensitive to many atomic-scale details because of Gaussian smoothing. Accurate approximations to the potential $\mathcal{V}_R(\mathbf{r})$ may then be obtained by using simple approximations for the solvent charge density that satisfy the exact long wavelength Stillinger–Lovett moment conditions (34), like those obtained from Debye–Hückel theory, $\rho_D^q(\mathbf{r}) = Qf_D(r)$ (35). As shown in *Supporting Information*, this approximation yields

$$\Delta G_{LMF} \approx -\frac{Q^2}{2}\int d\mathbf{r}\int d\mathbf{r}' f_D(\mathbf{r}) f_D(\mathbf{r}') v_1(|\mathbf{r}-\mathbf{r}'|) \qquad [14]$$

$$\sim -\frac{Q^2}{\epsilon\sigma\sqrt{\pi}}. \qquad [15]$$

Eq. **14** captures the behavior of ΔG_{LMF} with surprising accuracy, even though classic mean field theories using the Debye charge density are unable to produce overcharging (23). The simple Eq. **15** is equivalent to the self-interaction term of ref. 36 and highlights the quadratic dependence of ΔG_{LMF} on Q and its inverse dependence on σ. Although it is very accurate in many cases involving small ionic solutes (36), we find it to be only qualitatively accurate for this highly charged system.

The use of simple theoretical constructs in Eq. **14** that capture only a few long wavelength properties illustrates how LMF theory can be used in combination with existing frameworks to obtain both qualitative insight and accurate predictions.

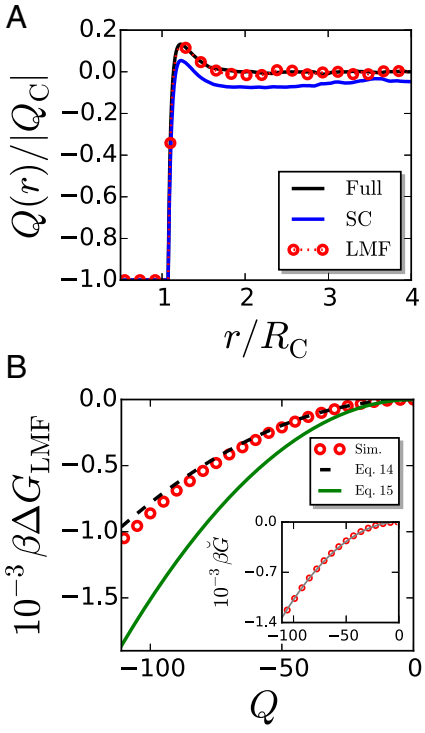

Fig. 4. (*A*) The integrated charge per unit colloid charge as a function of distance from the center of the colloid. (*B*) The LMF theory contribution to the solvation free energy as a function of the colloid charge. Data points indicate simulation results, the dashed line corresponds to a numerical integration of Eq. **14**, and the solid line corresponds to the prediction of Eq. **15**. (*Inset*) $\tilde{G}(Q)$ and a parabolic fit shown as a dashed line.

Conclusions and Outlook

In this paper we have shown that LMF theory quantitatively describes both the structure and thermodynamics of solvation in general molecular systems using only short-ranged models. Moreover, this enables the study of nonneutral systems, as illustrated in *Supporting Information*, by the estimation of an ion hydration free energy. We expect our approach to be of significant importance to the study of large biomolecular and materials systems, where poor scaling of lattice summation techniques (19) limits the length and time scales accessible to simulations [the most efficient particle-mesh algorithms for lattice summations scale like $N \log N$ with a large prefactor, where N is the number of particles in the system (17)]. Models with only short-ranged interactions scale linearly with system size, so the use of LMF theory

in conjunction with highly optimized biomolecular simulation packages should allow researchers to study length and time scales previously inaccessible without any loss in accuracy. Moreover, LMF theory can be used with commodity hardware such as graphics processing units without the need for additional algorithm development (37), offering another source of increased efficiency.

The general theoretical framework presented here is not limited to simple solvation and can be used to determine generic free energies as a function of an arbitrary order parameter by recasting more complex processes in the language of solvation (3). Thus, we expect this theory of solvation to find wide use and significantly affect free energy computations across molecular science.

Materials and Methods

Simulation Details. All simulations were performed with the DL_POLY 2.18 software package appropriately modified to incorporate the various interaction potentials used throughout this work (38). In the full systems, electrostatic interactions were evaluated using Ewald summation (17). Unless otherwise noted, LJ interactions and the real space part of the electrostatic interactions were truncated at 9 Å. Simulations were performed in the isobaric-isothermal (constant NPT) ensemble to ensure that the bulk density far from the solute remains constant across all systems.

Hard Sphere Solvation in an LJ Fluid and Water. Hard spheres were modeled as the WCA repulsive portion of an integrated, "9-3" LJ potential following previous work (27). To compute free energies, simulations were performed with repulsive spheres of varying radii, in increments of $\Delta R_{\mathrm{HS}} = 0.5$ Å, where the radius R_{HS} of the solute is given by the effective hard sphere diameter (7, 27). Free energies were then computed from energy differences between neighboring R_{HS} values using BAR (27, 39). The LJ fluid was simulated at a state near liquid–vapor coexistence, $T^* = 0.85$ and $P^* = 0.022$ in reduced units. Water was described using the SPC/E model, which adequately captures properties relevant to the description of hydrophobic hydration, including the isothermal compressibility and surface tension of water. Simulations of the SPC/E model were performed at $T = 300$ K and $P = 0$ atm, and the pressure in the GT system was appropriately corrected to yield the same density as the full system (28, 31).

Colloid Solvation Free Energy Calculations. Solvation free energies of purely repulsive spheres in the electrolyte solution were computed in analogy to those in water and the LJ fluid. To compute the charging free energy, we vary the charge on the colloid in increments of $\Delta Q = 1$ and use a "semigrand ensemble" to maintain the neutrality of the system at each value of Q by varying the number of coions between simulations performed in the NPT ensemble with $T = 298$ K and $P = 7.37$ atm. We justify this by noting that the colloid charge is neutralized by the solvent at a distance relatively close to the solute. Thus, the solution far from the solute can be considered a neutral reservoir, and adding coions when increasing Q is equivalent to pulling them from this reservoir of constant neutrality. The charging free energy was then evaluated using BAR (39). All colloid simulations were performed with a constant dielectric constant of $\epsilon = 78$.

Derivation of the Far-Field Solvation Free Energy. We derive an exact expression for the solvation free energy difference in the Grand ensemble $\check{\Omega}[\phi] - \check{\Omega}_{\mathrm{R}}[\phi_{\mathrm{R}}] \equiv \Delta\Omega_{\mathrm{LMF}}[\phi_{\mathrm{R}}]$ indicated by the green arrows in Fig. 1. We choose a path along the cycle where the slowly varying long-ranged portion $u_1(r)$ of the solvent intermolecular potential is linearly coupled by a parameter λ,

$$u_\lambda(r) \equiv u_0(r) + \lambda u_1(r). \tag{16}$$

The solute–solvent field $\phi_\lambda(\mathbf{r})$ also has a particular λ dependence to be specified later, such that when $\lambda = 0$, $\phi_\lambda = \phi_{\mathrm{R}}$ and when $\lambda = 1$, $\phi_\lambda = \phi$. The chemical potential μ_λ is chosen so that the pure solvent has the same density ρ_{B} for all λ.

The grand partition function at a particular value of λ can then be written as

$$\Xi_\lambda = \mathrm{Tr}\left\{ e^{-\beta\left[\mathcal{H}_\lambda(\overline{\mathbf{R}}_N) - N\mu_\lambda\right]} \right\}, \tag{17}$$

where $\mathrm{Tr}\{\cdot\} \equiv \sum_N [N!\Lambda^{3N}]^{-1} \int d\overline{\mathbf{R}}_N \{\cdot\}$ indicates the classical trace, Λ is the usual de Broglie wavelength, and $\overline{\mathbf{R}}_N \equiv \{\mathbf{r}_1, \mathbf{r}_2, \ldots, \mathbf{r}_N\}$ is a point in configuration space (40). Here

$$\mathcal{H}_\lambda(\overline{\mathbf{R}}_N) = \Phi_\lambda(\overline{\mathbf{R}}_N) + U_0(\overline{\mathbf{R}}_N) + \lambda U_1(\overline{\mathbf{R}}_N), \tag{18}$$

where $U_0(\overline{\mathbf{R}}_N)$ and $U_1(\overline{\mathbf{R}}_N)$ are total energies in configuration $\overline{\mathbf{R}}_N$ from the short- and long-ranged components of the solvent–solvent intermolecular potentials and $\Phi_\lambda(\overline{\mathbf{R}}_N) = \sum_i \phi_\lambda(\mathbf{r}_i)$ is the total energy from the solute–solvent field.

In the following it is useful to rewrite the solute–solvent energy and chemical potential terms in Eq. **17** using the microscopic configurational density

$$\rho(\mathbf{r}; \overline{\mathbf{R}}_N) \equiv \sum_{i=1}^{N} \delta(\mathbf{r} - \mathbf{r}_i) \tag{19}$$

as

$$\Phi_\lambda(\overline{\mathbf{R}}_N) - N\mu_\lambda = \int d\mathbf{r} [\phi_\lambda(\mathbf{r}) - \mu_\lambda] \rho(\mathbf{r}; \overline{\mathbf{R}}_N). \tag{20}$$

By differentiating the grand free energy $-\beta\Omega[\phi_\lambda] \equiv \ln \Xi_\lambda$ with respect to λ, we immediately obtain a well-known exact result

$$\frac{\partial\Omega[\phi_\lambda]}{\partial\lambda} = \int d\mathbf{r} \frac{d[\phi_\lambda(\mathbf{r}) - \mu_\lambda]}{d\lambda} \rho_\lambda(\mathbf{r}) + \frac{1}{2} \int d\mathbf{r} \int d\mathbf{r}' \rho_\lambda^{(2)}(\mathbf{r}, \mathbf{r}') u_1(|\mathbf{r} - \mathbf{r}'|). \tag{21}$$

Here $\rho_\lambda(\mathbf{r})$ and $\rho_\lambda^{(2)}(\mathbf{r}, \mathbf{r}')$ are the singlet and pair distribution functions in the nonuniform system with coupling parameter λ. We have assumed that $U_1(\overline{\mathbf{R}}_N)$ is given by a sum of pairwise interactions as in Eq. **16** and note from Eqs. **17**–**20** that

$$\rho_\lambda(\mathbf{r}) = \langle \rho(\mathbf{r}; \overline{\mathbf{R}}_N) \rangle_\lambda = \delta\Omega[\phi_\lambda] / \delta[\phi_\lambda(\mathbf{r}) - \mu_\lambda]. \tag{22}$$

We now integrate over λ to obtain the free energy difference between the mimic system at $\lambda = 0$ and the full system at $\lambda = 1$. Because the singlet densities at the endpoints are supposed to be equal by definition of the LMF, it is particularly useful to choose the λ dependence of $\phi_\lambda(\mathbf{r})$ and μ_λ such that the singlet density remains unchanged for all λ, $\rho_\lambda(\mathbf{r}) = \rho(\mathbf{r})$ (40, 41). Integrating Eq. **21** over this special path yields

$$\Omega[\phi] - \Omega_{\mathrm{R}}[\phi_{\mathrm{R}}] = \int d\mathbf{r} \rho(\mathbf{r}) [\phi(\mathbf{r}) - \mu - \phi_{\mathrm{R}}(\mathbf{r}) + \mu_{\mathrm{R}}] + \frac{1}{2} \int_0^1 d\lambda \int d\mathbf{r} \int d\mathbf{r}' \rho_\lambda^{(2)}(\mathbf{r}, \mathbf{r}') u_1(|\mathbf{r} - \mathbf{r}'|). \tag{23}$$

Eq. **23** gives the free energy difference associated with the rightmost green arrow in Fig. 1. The free energy of the remaining green arrow is obtained when $\phi = \phi_{\mathrm{R}} = 0$.

Because the solvation free energy is $\check{\Omega}[\phi] \equiv \Omega[\phi] - \Omega[\phi = 0]$, we can use Eq. **23** to write

$$\check{\Omega}[\phi] - \check{\Omega}_{\mathrm{R}}[\phi_{\mathrm{R}}] = -\int d\mathbf{r} \rho(\mathbf{r}) [\phi_{\mathrm{R}}(\mathbf{r}) - \phi(\mathbf{r})] + \int d\mathbf{r} [\rho(\mathbf{r}) - \rho_{\mathrm{B}}][\mu_{\mathrm{R}} - \mu] + \frac{1}{2} \int_0^1 d\lambda \int d\mathbf{r} \int d\mathbf{r}' \left[\rho_\lambda^{(2)}(\mathbf{r}, \mathbf{r}') - \rho_{\mathrm{B},\lambda}^{(2)}(|\mathbf{r} - \mathbf{r}'|) \right] u_1(|\mathbf{r} - \mathbf{r}'|), \tag{24}$$

with $\rho_{\mathrm{B},\lambda}^{(2)}(r)$ the pair distribution function in the pure solvent.

Eq. **24** is an exact formula for the solvation free energy difference corresponding to the green vertical arrows in Fig. 1. However, it may seem too complicated for practical use because it requires exact values of μ_{R} and μ and of the partially coupled nonuniform pair distribution function $\rho_\lambda^{(2)}(\mathbf{r}, \mathbf{r}')$. This in general is a function of six spatial variables and will vary with λ even though the nonuniform singlet density does not change along the chosen path.

However, we show here that when LMF theory provides an accurate self-consistent description of the induced single particle density $\rho(\mathbf{r})$ and associated LMF field $\phi_{\mathrm{R}}(\mathbf{r})$, we can obtain a very simple and accurate approximation to Eq. **24** involving only $\phi_{\mathrm{R}}(\mathbf{r})$ and $\rho(\mathbf{r})$. To that end, we note that the first two terms on the right generate a Legendre transform to the intrinsic free energy functional $\mathcal{F}$ widely used in classic density functional theories of fluids (11):

$$\mathcal{F}[\rho] \equiv \Omega[\phi] - \int d\mathbf{r} \rho(\mathbf{r}) [\phi(\mathbf{r}) - \mu]. \tag{25}$$

$\mathcal{F}$ is a functional of the conjugate induced density $\rho(\mathbf{r})$ and by elementary properties of the Legendre transform we have in analogy to Eq. **22** the exact result

$$\delta\mathcal{F}[\rho] / \delta\rho(\mathbf{r}) = -[\phi(\mathbf{r}) - \mu]. \tag{26}$$

Eq. **24** can then be exactly rewritten (41) as

$$\breve{\mathcal{F}}[\rho]-\breve{\mathcal{F}}_{\mathrm{R}}[\rho]=\frac{1}{2}\int_0^1 d\lambda\int d\mathbf{r}\int d\mathbf{r}'\left[\rho_\lambda^{(2)}(\mathbf{r},\mathbf{r}')-\rho_{\mathrm{B},\lambda}^{(2)}(|\mathbf{r}-\mathbf{r}'|)\right]u_1(|\mathbf{r}-\mathbf{r}'|). \quad [27]$$

The free energies in Eq. **27** are all functionals of the common density $\rho(\mathbf{r})=\rho_\lambda(\mathbf{r})=\rho_{\mathrm{R}}(\mathbf{r})$ because of the integration path we have chosen.

Using Eq. **26** we can functionally differentiate Eq. **27** to obtain a formally exact relation between $\phi_{\mathrm{R}}(\mathbf{r})$ and $\phi(\mathbf{r})$:

$$\phi_{\mathrm{R}}(\mathbf{r})=\phi(\mathbf{r})+\frac{\delta}{\delta\rho(\mathbf{r})}\times\left\{\frac{1}{2}\int_0^1 d\lambda\int d\mathbf{r}\int d\mathbf{r}'\left[\rho_\lambda^{(2)}(\mathbf{r},\mathbf{r}')-\rho_{\mathrm{B},\lambda}^{(2)}(|\mathbf{r}-\mathbf{r}'|)\right]u_1(|\mathbf{r}-\mathbf{r}'|)+\int d\mathbf{r}[\rho(\mathbf{r})-\rho_{\mathrm{B}}][\mu_{\mathrm{R}}-\mu]\right\}. \quad [28]$$

Here we have moved the chemical potentials terms inside the curly braces and chosen constants so the term inside the braces vanishes for a uniform bulk system where $\phi(\mathbf{r})=\phi_{\mathrm{R}}(\mathbf{r})=0$ and $\rho(\mathbf{r})=\rho_{\mathrm{B}}$.

The LMF Eq. **4**, derived independently by an approximate integration of the first member of the YBG hierarchy of equations relating intermolecular forces to induced structure (14, 21), gives a separate and often very accurate relation between $\phi_{\mathrm{R}}(\mathbf{r})$ and $\phi(\mathbf{r})$. This can be exactly rewritten in a form analogous to Eq. **28** as

$$\phi_{\mathrm{R}}(\mathbf{r})=\phi(\mathbf{r})+\frac{\delta}{\delta\rho(\mathbf{r})}\left\{\frac{1}{2}\int d\mathbf{r}\int d\mathbf{r}'[\rho(\mathbf{r})-\rho_{\mathrm{B}}][\rho(\mathbf{r}')-\rho_{\mathrm{B}}]u_1(|\mathbf{r}-\mathbf{r}'|)\right\}, \quad [29]$$

where constants have again been chosen such that the term in the curly braces vanishes in the uniform bulk. Using the LMF Eq. **4** the term in braces can be exactly rewritten as

$$\frac{1}{2}\int d\mathbf{r}\int d\mathbf{r}'[\rho(\mathbf{r})-\rho_{\mathrm{B}}][\rho(\mathbf{r}')-\rho_{\mathrm{B}}]u_1(|\mathbf{r}-\mathbf{r}'|)=\frac{1}{2}\int d\mathbf{r}[\rho(\mathbf{r})-\rho_{\mathrm{B}}][\phi_{\mathrm{R}}(\mathbf{r})-\phi(\mathbf{r})]. \quad [30]$$

Assuming the accuracy of the LMF approximation for $\phi_{\mathrm{R}}(\mathbf{r})$ and $\rho(\mathbf{r})$ we now subtract Eq. **29** from Eq. **28**. The potential terms cancel and we can then formally perform functional integrals over $\rho(\mathbf{r})$. Using Eq. **30** we obtain

$$\frac{1}{2}\int_0^1 d\lambda\int d\mathbf{r}\int d\mathbf{r}'\left[\rho_\lambda^{(2)}(\mathbf{r},\mathbf{r}')-\rho_{\mathrm{B},\lambda}^{(2)}(|\mathbf{r}-\mathbf{r}'|)\right]u_1(|\mathbf{r}-\mathbf{r}'|)+\int d\mathbf{r}[\rho(\mathbf{r})-\rho_{\mathrm{B}}][\mu_{\mathrm{R}}-\mu]=\frac{1}{2}\int d\mathbf{r}[\rho(\mathbf{r})-\rho_{\mathrm{B}}][\phi_{\mathrm{R}}(\mathbf{r})-\phi(\mathbf{r})]. \quad [31]$$

Thus, when using a properly chosen mimic system, the complicated expression on the left side of Eq. **31** involving the λ-dependent nonuniform pair distribution functions and exact values of μ and μ_{R} can be very accurately approximated by the simple expression on the right where only nonuniform singlet densities and the LMF appear!

The terms on the left side of Eq. **31** are the last two terms in the exact expression for the solvation free energy in Eq. **24**. Thus, it can be accurately approximated as

$$\breve{\Omega}[\phi]-\breve{\Omega}_{\mathrm{R}}[\phi_{\mathrm{R}}]=-\int d\mathbf{r}\rho(\mathbf{r})[\phi_{\mathrm{R}}(\mathbf{r})-\phi(\mathbf{r})]+\frac{1}{2}\int d\mathbf{r}\,[\rho(\mathbf{r})-\rho_{\mathrm{B}}][\phi_{\mathrm{R}}(\mathbf{r})-\phi(\mathbf{r})]=-\frac{1}{2}\int d\mathbf{r}\,[\rho(\mathbf{r})+\rho_{\mathrm{B}}][\phi_{\mathrm{R}}(\mathbf{r})-\phi(\mathbf{r})], \quad [32]$$

which is the basic LMF solvation formula Eq. **11**.

Eq. **32** requires the accuracy of the LMF Eq. **4** and exploits its simple mean field form in the "bottom-up" functional integration that gives the associated free energy change. This strongly contrasts with the usual treatment of mean field theory in classic DFT (11). In this "top-down" approach the free energy itself including constant terms is expressed as a general functional of the nonuniform density. It then is written as a sum of reference and perturbation parts, with the reference part often chosen for convenience as a hard sphere system for which accurate analytic functionals have been developed. This initial choice fixes the form of the remaining potential u_1 appearing in the perturbation part. A second crude "mean field approximation" where nonuniform pair distribution functions are replaced by the product of single particle functions is then typically used to simplify the perturbation term.

However, this DFT perspective provides no physical insight into what reference system should be used or when and why the mean field product approximation would be expected to be accurate. Nevertheless, as noted by Archer and Evans (42) (AE), when the crude mean field approximation is used and the associated single particle potential is calculated by functional derivatives as in Eq. **26**, one obtains an equation very similar to the LMF Eq. **4**. Indeed, AE assert that the LMF equation "follows directly from the standard mean-field DFT treatment of attractive forces."

However, the detailed derivation of the LMF equation from the YBG hierarchy in ref. 21 and *Supporting Information* makes no use of the crude mean field approximation or other concepts from DFT. It shows that the resulting mean field form and quantitive accuracy requires a well chosen u_1 that remains slowly varying over characteristic nearest-neighbor distances. Satisfying this constraint is particularly problematic when trying to use DFT for charged and polar systems. As illustrated here, an accurate short-ranged mimic system must then generally include the short-ranged parts of the Coulomb interactions as well as the (hard sphere-like) repulsive core interactions. It seems unlikely that accurate analytic free energy functionals for such complicated reference systems can ever be developed.

As emphasized in ref. 21, the LMF equation (and in particular its use here to obtain solvation free energies) "is not a blind assertion of mean-field behavior but rather a controlled and accurate approximation, provided that we choose our mimic system carefully." See *Supporting Information* for further discussion of this important point and a detailed derivation of the LMF equation.

ACKNOWLEDGMENTS. We thank Jocelyn Rodgers, Zhonghan Hu, and Giacomo Fiorin for helpful comments on the manuscript. This work was supported by National Science Foundation Grants CHE0848574 and CHE1300993.

1. Levy Y, Onuchic JN (2006) Water mediation in protein folding and molecular recognition. *Annu Rev Biophys Biomol Struct* 35:389–415.
2. Dill KA (1990) Dominant forces in protein folding. *Biochemistry* 29(31): 7133–7155.
3. Chipot C, Pohorille A, eds (2007) *Free Energy Calculations: Theory and Applications in Chemistry and Biology* (Springer, Berlin).
4. Venkateshwaran V, Vembanur S, Garde S (2014) Water-mediated ion-ion interactions are enhanced at the water vapor-liquid interface. *Proc Natl Acad Sci USA* 111(24): 8729–8734.
5. Born M (1920) Volumes and hydration warmth of ions. *Z Phys* 1:45–48.
6. Widom B (1967) Intermolecular forces and the nature of the liquid state: Liquids reflect in their bulk properties the attractions and repulsions of their constituent molecules. *Science* 157(3787):375–382.
7. Weeks JD, Chandler D, Andersen HC (1971) Role of repulsive forces in determining the equilibrium structure of simple liquids. *J Chem Phys* 54:5237–5247.
8. Pratt LR, Chandler D (1977) Theory of the hydrophobic effect. *J Chem Phys* 67: 3683–3704.
9. Stillinger FH (1973) Structure in aqueous solutions of nonpolar solutes from the standpoint of scaled-particle theory. *J Solution Chem* 2:141–158.
10. Widom B (1982) Potential-distribution theory and the statistical mechanics of fluids. *J Phys Chem* 86:869–872.
11. Evans R (1992) *Fundamentals of Inhomogenous Fluids*, ed Henderson D (Dekker, New York).
12. Hummer G, Garde S, García AE, Pohorille A, Pratt LR (1996) An information theory model of hydrophobic interactions. *Proc Natl Acad Sci USA* 93(17):8951–8955.
13. Lum K, Chandler D, Weeks JD (1999) Hydrophobicity at small and large length scales. *J Phys Chem B* 103:4570–4577.
14. Weeks JD (2002) Connecting local structure to interface formation: A molecular scale van der Waals theory of nonuniform liquids. *Annu Rev Phys Chem* 53:533–562.
15. Ashbaugh HS, Pratt LR (2006) Colloquium: Scaled particle theory and the length scales of hydrophobicity. *Rev Mod Phys* 78:159–178.
16. Beck TL, Paulaitis ME, Pratt LR (2006) *The Potential Distribution Theorem and Models of Molecular Solutions* (Cambridge Univ Press, Cambridge, UK).
17. Allen MP, Tildesley DJ (1987) *Computer Simulation of Liquids* (Oxford, New York).
18. Figueiredo F, Buono GSD, Levy RM (1995) On finite-size effects in computer simulations using the Ewald potential. *J Chem Phys* 103:6133–6142.
19. Schulz R, Lindner B, Petridis L, Smith JC (2009) Scaling of multimillion-atom biological molecular dynamics simulation on a petascale computer. *J Chem Theory Comput* 5(10):2798–2808.
20. Hünenberger PH, McCammon JA (1999) Effect of artificial periodicity in simulations of biomolecules under Ewald boundary conditions: a continuum electrostatics study. *Biophys Chem* 78(1-2):69–88.
21. Rodgers JM, Weeks JD (2008) Local molecular field theory for the treatment of electrostatics. *J Phys Condens Matter* 20:494206.
22. Moreira A, Netz R (2002) Strong-coupling theory for counter-ion distributions. *Europhys Lett* 52:705–711.

23. Levin Y (2002) Electrostatic correlations: from plasma to biology. *Rep Prog Phys* 65:1577–1632.
24. Hu Z (2014) Symmetry-preserving mean field theory for electrostatics at interfaces. *Chem Commun (Camb)* 50(92):14397–14400.
25. Beck TL (2011) Hydration free energies by energetic partitioning of the potential distribution theorem. *J Stat Phys* 145:335–354.
26. Hu Z, Weeks JD (2010) Efficient solutions of self-consistent mean field equations for dewetting and electrostatics in nonuniform liquids. *Phys Rev Lett* 105(14):140602.
27. Remsing RC, Weeks JD (2013) Dissecting hydrophobic hydration and association. *J Phys Chem B* 117(49):15479–15491.
28. Remsing RC, Rodgers JM, Weeks JD (2011) Deconstructing classical water models at interfaces and in bulk. *J Stat Phys* 145:313–334.
29. Chandler D (2005) Interfaces and the driving force of hydrophobic assembly. *Nature* 437(7059):640–647.
30. Rodgers JM, Weeks JD (2008) Interplay of local hydrogen-bonding and long-ranged dipolar forces in simulations of confined water. *Proc Natl Acad Sci USA* 105(49):19136–19141.
31. Rodgers JM, Weeks JD (2009) Accurate thermodynamics for short-ranged truncations of Coulomb interactions in site-site molecular models. *J Chem Phys* 131(24):244108.
32. Remsing RC, Weeks JD (2015) Hydrophobicity scaling of aqueous interfaces by an electrostatic mapping. *J Phys Chem B* 119(29):9268–9277.
33. Diehl A, Levin Y (2006) Smoluchowski equation and the colloidal charge reversal. *J Chem Phys* 125(5):054902.
34. Stillinger FH, Lovett R (1968) General restriction on the distribution of ions in electrolytes. *J Chem Phys* 49:1991–1994.
35. Denesyuk NA, Weeks JD (2008) A new approach for efficient simulation of Coulomb interactions in ionic fluids. *J Chem Phys* 128(12):124109.
36. Hummer G, Pratt LR, García AE (1996) Free energy of ionic hydration. *J Phys Chem* 100:1206–1215.
37. Götz AW, et al. (2012) Routine microsecond molecular dynamics simulations with AMBER on GPUs. 1. Generalized Born. *J Chem Theory Comput* 8(5):1542–1555.
38. Smith W, Yong C, Rodger P (2002) DL_POLY: Application to molecular simulation. *Mol Simul* 28:385–471.
39. Bennett CH (1976) Efficient estimation of free energy differences from monte carlo data. *J Comput Phys* 22:245–268.
40. Weeks JD (2003) External fields, density functionals, and the Gibbs inequality. *J Stat Phys* 110:1209–1217.
41. Weeks JD, Bedeaux D, Zielinska BJA (1984) Anisotropic van der waals model of the liquid-vapor interface. *J Chem Phys* 80:3790–3800.
42. Archer AJ, Evans R (2013) Relationship between local molecular field theory and density functional theory for non-uniform liquids. *J Chem Phys* 138(1):014502.
43. Kac M, Uhlenbeck GE, Hemmer PC (1963) On the van der waals theory of the vapor-liquid equilibrium. i. discussion of a one-dimensional model. *J Math Phys* 4:216–228.
44. Sokolowski S, Fischer J (1992) The role of attractive intermolecular forces in the density functional theory of inhomogeneous fluids. *J Chem Phys* 96:5441–5447.
45. Tang Z, Scriven LE, Davis HT (1991) Density-functional perturbation theory of inhomogeneous simple fluids. *J Chem Phys* 95:2659–2668.
46. Chaudhari MI, Rempe SB, Asthagiri D, Tan L, Pratt LR (2015) Molecular theory for the effects of solute attractive forces on hydrophobic interactions. arXiv:1501.02495v1.
47. Hummer G, Soumpasis DM (1993) Correlation and free energies in restricted primitive model descriptions of electrolytes. *J Chem Phys* 98:581–591.

Supporting Information

Remsing et al. 10.1073/pnas.1521570113

Derivation of the LMF Equation and Relation to DFT

For simplicity we consider solvation in a simple one-component LJ-like system, although these ideas can be readily extended to Coulomb systems, using methods described in ref. 21. LMF theory and most perturbation approaches based on classic DFT consider a restricted class of density-matched reference systems, denoted here by a subscript $\tilde{\mathrm{R}}$, with pair potential $u_0(r)$ where a special effective solute field $\phi_{\tilde{\mathrm{R}}}(\mathbf{r})$ is chosen such that the induced density equals that of the full system (11, 14, 40):

$$\rho_{\tilde{\mathrm{R}}}(\mathbf{r};[\phi_{\tilde{\mathrm{R}}}]) = \rho(\mathbf{r};[\phi]). \qquad \text{[S1]}$$

Here we have explicitly indicated the functional dependence of the densities on their respective fields, but this will be omitted in what follows unless needed for clarity. The tilde in $\tilde{\mathrm{R}}$ emphasizes that the value of $\phi_{\tilde{\mathrm{R}}}(\mathbf{r})$ depends strongly on the so-far-unspecified choice of $u_0(r)$ in the reference system.

As would be expected, the utility and accuracy of any simple perturbation approach requires a well-chosen reference $u_0(r)$. It is very plausible that such a $\phi_{\tilde{\mathrm{R}}}(\mathbf{r})$ exists for any reasonable choice of $u_0(r)$, especially when $u_0(r)$ captures most of the strong short-ranged intermolecular forces. However, in principle, one could even choose a density-matched ideal gas reference system with $u_0(r) = 0$, as is done in standard DFT approaches (11) to define the one body and higher-order direct correlation functions as functional derivatives of the excess free energy functional.

LMF theory uses the exact YBG hierarchy of equations relating liquid structure and forces to derive a formally exact equation satisfied by $\phi_{\tilde{\mathrm{R}}}(\mathbf{r})$ (14, 21). The first equation in the hierarchy for the full system can be written as

$$-\vec{\nabla}\ln\rho(\mathbf{r}) = \beta\vec{\nabla}\phi(\mathbf{r}) + \int d\mathbf{r}'\rho(\mathbf{r}'|\mathbf{r})\beta\vec{\nabla}u(|\mathbf{r}-\mathbf{r}'|). \qquad \text{[S2]}$$

Here $\rho(\mathbf{r}'|\mathbf{r})$ is the conditional density, the average density at position $\mathbf{r}'$ given that a particle is at $\mathbf{r}$, and is defined in terms of the pair distribution function as

$$\rho(\mathbf{r}'|\mathbf{r}) \equiv \frac{\rho^{(2)}(\mathbf{r},\mathbf{r}')}{\rho(\mathbf{r})}. \qquad \text{[S3]}$$

A key step in deriving the LMF equation is to subtract from Eq. **S2** the analogous YBG equation for a density matched reference system (14, 21). Using Eq. **S1** we find exactly

$$\vec{\nabla}\phi_{\tilde{\mathrm{R}}}(\mathbf{r}) = \vec{\nabla}\phi(\mathbf{r}) + \int d\mathbf{r}'\rho(\mathbf{r}'|\mathbf{r})\vec{\nabla}u(|\mathbf{r}-\mathbf{r}'|) - \int d\mathbf{r}'\rho_{\tilde{\mathrm{R}}}(\mathbf{r}'|\mathbf{r})\vec{\nabla}u_0(|\mathbf{r}-\mathbf{r}'|). \qquad \text{[S4]}$$

This result can be exactly written in a form useful for further analysis as

$$\vec{\nabla}\phi_{\tilde{\mathrm{R}}}(\mathbf{r}) = \vec{\nabla}\phi(\mathbf{r}) + \int d\mathbf{r}'\rho_{\tilde{\mathrm{R}}}(\mathbf{r}')\vec{\nabla}u_1(|\mathbf{r}-\mathbf{r}'|) \qquad \text{[S5]}$$

$$+ \int d\mathbf{r}'\left[\rho(\mathbf{r}'|\mathbf{r}) - \rho_{\tilde{\mathrm{R}}}(\mathbf{r}'|\mathbf{r})\right]\vec{\nabla}u_0(|\mathbf{r}-\mathbf{r}'|) \qquad \text{[S6]}$$

$$+ \int d\mathbf{r}'[\rho(\mathbf{r}'|\mathbf{r}) - \rho(\mathbf{r}')]\vec{\nabla}u_1(|\mathbf{r}-\mathbf{r}'|). \qquad \text{[S7]}$$

Eq. **S4** formally determines $\phi_{\tilde{\mathrm{R}}}(\mathbf{r})$ for any choice of $u_0(r)$, $u_1(r)$, and $\phi(\mathbf{r})$. However, because conditional densities that involve complicated nonuniform pair correlation functions still appear, it is generally not very useful in practical calculations.

As argued in detail in ref. 21, considerable simplifications arise when we can choose an optimal separation where the short-ranged $u_0(r)$ has essentially the same strong short-ranged forces at characteristic nearest-neighbor distances as in the full potential along with a corresponding $u_1(r)$ that is very slowly varying on that length scale. We call such a special density-matched reference system a mimic system and denote it by the subscript R.

These common strong forces should generate very similar features in the conditional densities in both the full and mimic systems at short length scales where $\vec{\nabla}u_0$ is nonzero so it is plausible that Eq. **S6** is small. Similarly the gradient of the slowly varying u_1 in Eq. **S7** is small at short distances, precisely the region where the conditional and singlet densities differ most from each other. At larger distances, assuming there are no intrinsic long-ranged correlations as seen near critical points, and so on, the conditional and singlet densities approach one another and the integrand is again small. Thus, in many cases the term **S7** is also very small.

To derive the LMF equation we assume both terms can be neglected. The remaining term **S5** can then be integrated exactly. Imposing the boundary condition that the density reduces to ρ_{B} far from the solute or when $\phi \to 0$ then gives the LMF equation for the mimic system:

$$\phi_{\mathrm{R}}(\mathbf{r}) = \phi(\mathbf{r}) + \int d\mathbf{r}'[\rho_{\mathrm{R}}(\mathbf{r}') - \rho_{\mathrm{B}}]u_1(|\mathbf{r}-\mathbf{r}'|). \qquad \text{[S8]}$$

The LMF equation has the form of a mean field equation that self-consistently relates the effective field ϕ_{R} to the nonuniform singlet density it induces. This derivation shows that this simple form can be expected to be accurate only for a well-chosen mimic system resulting from a uniformly slowly varying u_1. Strictly speaking the correction terms to the LMF equation exactly vanish only in the artificial "Kac-limit" with an infinitely slowly varying and long-ranged u_1 (43), so the accuracy of LMF theory in practice for realistic potentials must be carefully assessed. Further analysis and extensions of these ideas will also likely be needed to describe mixtures of mobile components with very different core sizes.

Fortunately, experience has shown that LMF theory gives very accurate results in many cases both for nonuniform LJ fluids with walls or fixed solutes, and even better results have been found for charged and polar systems by properly separating the Coulomb potential. When the accuracy of the LMF equation can be established, *Materials and Methods*, *Derivation of the Far-Field Solvation Free Energy* in the main text shows that simple and very accurate approximations for the solvation free energy can then be found by a "bottom-up" functional integration over the LMF potential and induced density.

Archer and Evans (42) (AE) have recently argued that DFT offers an alternate pathway to the LMF equation, asserting that it "follows directly from the standard mean-field DFT treatment of attractive forces." Here we simplify their argument and assess the validity of this statement.

The standard DFT perturbation treatment focuses directly on the intrinsic free energy functional $\mathcal{F}[\rho]$ for the full system defined in Eq. **25** of the main text and that of an appropriately chosen density matched reference system $\tilde{\mathrm{R}}$, writing

$$\mathcal{F}[\rho] = \mathcal{F}_{\tilde{\mathrm{R}}}[\rho] + \Delta\mathcal{F}_{\tilde{\mathrm{R}}}[\rho]. \qquad \textbf{[S9]}$$

In this "top-down" DFT approach the associated effective potentials and equilibrium correlation functions are then determined by functional derivatives of Eq. **S9** as in Eq. **26** of the main text.

In practice accurate analytic approximations for $\mathcal{F}_{\tilde{\mathrm{R}}}$ are known only for an ideal gas or a harshly repulsive hard sphere like reference system. Optimistically assuming that such an analytic reference system $\tilde{\mathrm{R}}$ can be chosen, we now focus on approximating the perturbation term $\Delta\mathcal{F}_{\tilde{\mathrm{R}}}[\rho]$. As in Eq. **27** of the main text, this can be exactly written as

$$\Delta\mathcal{F}_{\tilde{\mathrm{R}}}[\rho] = \frac{1}{2}\int_0^1 d\lambda \int d\mathbf{r} \int d\mathbf{r}' \rho_\lambda^{(2)}(\mathbf{r},\mathbf{r}') u_1(|\mathbf{r}-\mathbf{r}'|). \qquad \textbf{[S10]}$$

Although some workers have tried to simplify Eq. **S10** by replacing the nonuniform pair correlation function by that of a uniform system at some intermediate or averaged density (44, 45), it is not clear how this should be chosen in very nonuniform systems and the results depend strongly on the choice made.

By default, most researchers have used the crude but much simpler mean field approximation discussed by AE. For any density-matched reference system $\tilde{\mathrm{R}}$ where $\rho(\mathbf{r}) = \rho_\lambda(\mathbf{r}) = \rho_{\tilde{\mathrm{R}}}(\mathbf{r})$, this asserts that pair correlations in Eq. **S10** can be safely ignored by approximating

$$\rho_\lambda^{(2)}(\mathbf{r},\mathbf{r}') \equiv \rho(\mathbf{r})\rho(\mathbf{r}')g_\lambda(\mathbf{r},\mathbf{r}') \approx \rho_{\tilde{\mathrm{R}}}(\mathbf{r})\rho_{\tilde{\mathrm{R}}}(\mathbf{r}'). \qquad \textbf{[S11]}$$

Eq. **S9** then can be written as

$$\mathcal{F}[\rho] = \mathcal{F}_{\tilde{\mathrm{R}}}[\rho] + \frac{1}{2}\int d\mathbf{r} \int d\mathbf{r}' \rho_{\tilde{\mathrm{R}}}(\mathbf{r})\rho_{\tilde{\mathrm{R}}}(\mathbf{r}') u_1(|\mathbf{r}-\mathbf{r}'|). \qquad \textbf{[S12]}$$

Taking functional derivatives as in Eq. **26** of the main text we then have

$$\left[\phi_{\tilde{\mathrm{R}}}(\mathbf{r}) - \mu_{\tilde{\mathrm{R}}}\right] = [\phi(\mathbf{r}) - \mu] + \int d\mathbf{r}' \rho_{\tilde{\mathrm{R}}}(\mathbf{r}') u_1(|\mathbf{r}-\mathbf{r}'|). \qquad \textbf{[S13]}$$

When $\phi(\mathbf{r}) = \phi_{\tilde{\mathrm{R}}}(\mathbf{r}) = 0$, $\rho_{\tilde{\mathrm{R}}}(\mathbf{r}) = \rho_{\mathrm{B}}$ and Eq. **S13** reduces to the mean field van der Waals approximation for the bulk chemical potentials (14):

$$\mu = \mu_{\tilde{\mathrm{R}}} + \rho_{\mathrm{B}} \int d\mathbf{r}' u_1(|\mathbf{r}-\mathbf{r}'|). \qquad \textbf{[S14]}$$

Using this in Eq. **S13** and taking $\tilde{\mathrm{R}} = \mathrm{R}$ then gives an equation seemingly equivalent to the LMF Eq. **S8**, as noted by AE.

Although this and related derivations of an LMF-like equation may have the "advantage of concision" (46), we consider them quite misleading from a fundamental point of view. They seem to link the quantitative success of the LMF equation to the accuracy of the crude mean field approximation in **S11** or **S12**. However, the magnitude and nature of possible errors that this direct and uncontrolled imposition of a mean field form could induce both on the free energy itself and on correlation functions and fields given by functional derivatives of the approximate form are by no means obvious.

Closely related problems with the use of the crude mean field approximation are apparent even in the direct derivation of the LMF equation from the YBG hierarchy. If Eq. **S11** is used in the exact Eqs. **S5**–**S7**, the terms involving conditional densities vanish identically for any density matched reference system $\tilde{\mathrm{R}}$ and we seem to arrive at the LMF form for any such reference system. However, the detailed analysis of those terms shows that this conclusion can at best be justified only for a properly chosen mimic system $\tilde{\mathrm{R}} = \mathrm{R}$ and for states without intrinsic long-ranged correlations.

The LJ fluid represents one of the few cases where the mimic system can be well approximated by a hard sphere reference system and almost all quantitatively successful applications of the mean field approximation in DFT have been for the LJ fluid. However, it seems highly implausible even for the LJ fluid with a near-optimal WCA choice of reference system that the crude mean field approximation in Eq. **S12** could accurately reproduce the exact free energy in Eq. **S10** over a wide range of densities.

This is immediately clear for a uniform fluid where $\rho(\mathbf{r}) = \rho_{\mathrm{B}}$. Then Eq. **S9** reduces to the usual Helmholtz free energy F and Eq. **S10** gives the exact uniform fluid perturbation expression for ΔF_0 involving integration over $\rho_{\mathrm{B}}^2 g_\lambda(r)$. This equation played a key role in the development of the WCA perturbation theory for uniform fluids (7), where $\rho_{\mathrm{B}}^2 g_\lambda(r)$ was replaced in Eq. **S10** by its value at $\lambda = 0$, $\rho_{\mathrm{B}}^2 g_0(r)$. This can give quite accurate results for ΔF_0 at high densities with the WCA separation.

This approximation can be motivated by mean field ideas applied to structure and forces, where the net effects of the long-ranged attractive forces from u_1 on $g_\lambda(r)$ in typical configurations in a uniform LJ fluid can be argued to cancel to a good approximation (6, 7). LMF theory can be used to improve on this approximation for uniform fluids and extend these ideas to nonuniform fluids. However, direct use of the crude mean field approximation on the level of free energies essentially assumes there exists a generally accurate constant value of the background potential (the van der Waals "a" term) and attempts to determine its value while ignoring even g_0 correlations. Indeed when $\rho_{\mathrm{B}}^2 g_\lambda(r)$ is replaced by only by ρ_{B}^2 in Eq. **S10**, quantitative errors (14) ranging from 10 to 15 percent for ΔF_0 are found. There are similar errors of this magnitude for the van der Waals mean field expression for the chemical potential in Eq. **S14**.

LMF theory shows how and why the LMF equation and natural generalizations to Coulomb systems can nevertheless be used to give quantitatively accurate results for the structure induced by the solute and for the excess solvation thermodynamics both for the nonuniform LJ fluid and for a wide variety of charged and polar systems as well. However, its success in this particular context should not be taken as evidence for the more general validity of **S11** or **S12**.

Solvation in the Mimic System

To determine the solvation free energy in the mimic system, $\breve{\Omega}_{\mathrm{R}}[\phi_{\mathrm{R}}]$, we take advantage of the separation of interactions suggested by Eq. **9** of the main text. Thus, we write

$$\breve{\Omega}_{\mathrm{R}}[\phi_{\mathrm{R}}] = \breve{\Omega}_0[\phi_0] + \Delta\Omega_{\mathrm{R1}}[\phi_{\mathrm{R1}}], \qquad \textbf{[S15]}$$

where $\breve{\Omega}_0[\phi_0]$ is the free energy of solvating a purely short-ranged solute with known potential $\phi_0(\mathbf{r})$ in the SC system, and $\Delta\Omega_{\mathrm{R1}}[\phi_{\mathrm{R1}}]$ is the free energy of turning on the LMF correction $\phi_{\mathrm{R1}}(\mathbf{r})$, as illustrated in Fig. S1. The free energy $\breve{\Omega}_0$ can be determined through conventional means such as alchemical or umbrella sampling techniques (3) and in general will require multiple intermediate states, as suggested by the red arrow in Fig. S1.

The slowly varying nature of $\phi_{\mathrm{R1}}(\mathbf{r})$ over molecular length scales leads one to anticipate that its contribution to the total energy will follow Gaussian statistics to a good approximation. When this holds, $\Delta\Omega_{\mathrm{R1}}$ is accurately given by (3)

$$\Delta\Omega_{R1}[\phi_{R1}] \approx \frac{1}{2}\int d\mathbf{r}[\rho_R(\mathbf{r}) + \rho_0(\mathbf{r})]\phi_{R1}(\mathbf{r}). \quad \textbf{[S16]}$$

We find that the distributions of the slowly varying portion of the renormalized field are indeed remarkably Gaussian for all systems studied here; in special cases where these Gaussians do not overlap sufficiently, intermediate states can be used to ensure accuracy (3). Thus, Eq. **S16** provides a simple and accurate estimate of $\Delta\Omega_{R1}$, emphasized by the green arrow in Fig. S1.

Similar statements hold in the context of electrostatic interactions, enabling the estimation of the corresponding free energy due to turning on $\mathcal{V}_{R1}(\mathbf{r}) = \mathcal{V}_R(\mathbf{r}) - \mathcal{V}_0(\mathbf{r})$ within the Gaussian approximation,

$$\Delta\Omega_{R1}[\mathcal{V}_{R1}] \approx \frac{1}{2}\int d\mathbf{r}\left[\rho_R^q(\mathbf{r}) + \rho_0^q(\mathbf{r})\right]\mathcal{V}_{R1}(\mathbf{r}). \quad \textbf{[S17]}$$

Numerically Practical Form of the Long-Ranged Contribution to the Solvation Free Energy

There exists a cancellation of terms between the solvation free energy of the mimic system and Eq. **11** of the main text, clearly observed when using Eq. **S16**. Although the separation of free energy contributions in this manner is favorable for physical interpretation, such cancellations can lead to numerical inaccuracies in some contexts. To avoid such inaccuracies, we can combine Eq. **S16** with Eq. **11** of the main text to obtain a useful expression for the total long-ranged component of the solvation free energy, $\breve{\Omega}_1[\phi_{R1}] = \breve{\Omega}[\phi] - \breve{\Omega}_0[\phi_0]$:

$$\begin{aligned}\breve{\Omega}_1 = &\frac{1}{2}\int d\mathbf{r}[\rho(\mathbf{r}) + \rho_0(\mathbf{r})]\phi_1(\mathbf{r}) \\ &+ \frac{1}{2}\int d\mathbf{r}[\rho_0(\mathbf{r}) - \rho_B][\phi_R(\mathbf{r}) - \phi(\mathbf{r})],\end{aligned} \quad \textbf{[S18]}$$

where $\rho_0(\mathbf{r})$ is the nonuniform density in the SC reference system. Eq. **S18** removes the cancelling terms and thus is numerically advantageous when the Gaussian approximation is accurate.

For completeness, we note that the electrostatic analog of Eq. **S18** can be readily obtained by substituting charge densities for densities, as is done in ref. 21 for the LMF equation. This leads to

$$\breve{\Omega}_1[\mathcal{V}_R] = \frac{1}{2}\int d\mathbf{r}\left[\rho^q(\mathbf{r}) + \rho_0^q(\mathbf{r})\right]\mathcal{V}_1(\mathbf{r}) + \frac{1}{2}\int d\mathbf{r}\rho_0^q(\mathbf{r})[\mathcal{V}_R(\mathbf{r}) - \mathcal{V}(\mathbf{r})], \quad \textbf{[S19]}$$

where $\rho_0^q(\mathbf{r})$ is the charge density in the electrostatic SC system defined by the strong coupling solute field $\mathcal{V}_0(\mathbf{r})$.

Linear Response Theory for the Charge Density

In this section, we briefly review the linear response formalism of Hu and Weeks (26) for determining the charge density of the mimic system directly from a system with some effective slowly varying electrostatic potential $\tilde{\mathcal{V}}_{R1}(\mathbf{r})$. The SC system corresponds to $\tilde{\mathcal{V}}_{R1}(\mathbf{r}) = 0$, whereas the mimic system is obtained when $\tilde{\mathcal{V}}_{R1}(\mathbf{r}) = \mathcal{V}_{R1}(\mathbf{r})$. We first define the potential energy due to $\tilde{\mathcal{V}}_{R1}(\mathbf{r})$ in a configuration $\overline{\mathbf{R}}$ as

$$\Phi_{R1}(\overline{\mathbf{R}}) \equiv \sum_{i=1}^{N} q_i \tilde{\mathcal{V}}_{R1}(\mathbf{r}_i) \quad \textbf{[S20]}$$

$$= \int d\mathbf{r}\rho^q(\mathbf{r};\overline{\mathbf{R}})\tilde{\mathcal{V}}_{R1}(\mathbf{r}), \quad \textbf{[S21]}$$

where N is the number of charges in the system and $\rho^q(\mathbf{r};\overline{\mathbf{R}}) = \sum_{i=1}^{N} q_i\delta(\mathbf{r} - \mathbf{r}_i(\overline{\mathbf{R}}))$ is the instantaneous charge density.

We now determine $\rho_R^q(\mathbf{r}) = \langle\rho^q(\mathbf{r};\overline{\mathbf{R}})\rangle_{\mathcal{V}_{R1}}$, the charge density in the mimic system, from configurations obtained in the presence of $\tilde{\mathcal{V}}_{R1}(\mathbf{r})$. Typical density response theory estimates involve difficult and highly fluctuating averages over exponentials. Hu and Weeks (26) overcome this difficulty through the linear response estimate

$$\left\langle\rho^q(\mathbf{r};\overline{\mathbf{R}})\right\rangle_{\mathcal{V}_{R1}} \simeq \left\langle\rho^q(\mathbf{r};\overline{\mathbf{R}})\right\rangle_{\tilde{\mathcal{V}}_{R1}} - \beta\left\langle\delta\rho^q(\mathbf{r};\overline{\mathbf{R}})\delta\Phi_{R1}(\overline{\mathbf{R}})\right\rangle_{\tilde{\mathcal{V}}_{R1}}. \quad \textbf{[S22]}$$

Here,

$$\delta\rho^q(\mathbf{r};\overline{\mathbf{R}}) \equiv \rho^q(\mathbf{r};\overline{\mathbf{R}}) - \left\langle\rho^q(\mathbf{r};\overline{\mathbf{R}})\right\rangle_{\tilde{\mathcal{V}}_{R1}} \quad \textbf{[S23]}$$

and

$$\delta\Phi_{R1}(\overline{\mathbf{R}}) \equiv \Phi_{R1}(\overline{\mathbf{R}}) - \left\langle\Phi_{R1}(\overline{\mathbf{R}})\right\rangle_{\tilde{\mathcal{V}}_{R1}} \quad \textbf{[S24]}$$

are deviations in the charge density and net potential energy due to $\tilde{\mathcal{V}}_{R1}$ from their respective means.

The charge density around a repulsive sphere with radius $R_{HS} = 12$ Å is shown in Fig. S2*A* for the full, GT, and mimic (LMF) systems. The charge density in the mimic system was determined using Eq. **S22** with $\tilde{\mathcal{V}}_{R1}(\mathbf{r}) = 0$; that is, $\rho^q(\mathbf{r})$ was determined by using linear response theory on the configurations of the GT system whose charge density is also shown in Fig. S2*A*. The formalism of Hu and Weeks (26) corrects the charge density of the GT system with quantitative accuracy, bringing it into good agreement with that of the full system. The LMF potential $\mathcal{V}_{R1}(r)$ obtained in this manner is also shown in Fig. S2*B*.

Debye–Hückel Approximation for the LMF Free Energy Contribution to Colloid Solvation

The electrostatic LMF contribution to the solvation free energy is

$$\beta\Delta\Omega_{LMF}[\mathcal{V}_R] = -\frac{\beta}{2}\int d\mathbf{r}\rho^q(\mathbf{r})[\mathcal{V}_R(\mathbf{r}) - \mathcal{V}(\mathbf{r})]. \quad \textbf{[S25]}$$

The bracketed term corresponds to the renormalized portion of the LMF from solvent–solvent interactions,

$$\mathcal{V}_S(\mathbf{r}) \equiv \mathcal{V}_R(\mathbf{r}) - \mathcal{V}(\mathbf{r}) = \frac{1}{\epsilon}\int d\mathbf{r}'\rho^q(\mathbf{r}')v_1(|\mathbf{r} - \mathbf{r}'|). \quad \textbf{[S26]}$$

To proceed with our calculation, it is natural to transform to Fourier space. Using Parseval's theorem, the LMF term can be written as

$$\beta\Delta\Omega_{LMF}[\mathcal{V}_R] = -\frac{\beta}{2}\frac{1}{(2\pi)^3}\int d\mathbf{k}\hat{\rho}^q(\mathbf{k})\widehat{\mathcal{V}_S}(\mathbf{k}), \quad \textbf{[S27]}$$

where

$$\widehat{\mathcal{V}_S}(\mathbf{k}) = \frac{4\pi}{\epsilon k^2}e^{-k^2\sigma^2/4}\hat{\rho}^q(\mathbf{k}). \quad \textbf{[S28]}$$

Previous work has illustrated that simple approximations such as Debye–Hückel theory can be used to approximate the charge density in the LMF equation with great success (35). Such theories accurately describe the asymptotic behavior of charged systems, as described by the Stillinger–Lovett zeroth and second moment conditions (34, 35). Because LMF theory focuses on long-ranged, slowly varying interactions, structure (35) and thermodynamics (31) can be obtained with only an accurate description of the asymptotic behavior of the system. Therefore, we expect that a Debye–Hückel approximation to the charge density

will at least describe the qualitative behavior of the LMF contribution to the free energy.

The charge density of solvent ions can be written using Debye–Hückel theory as (35)

$$\rho_{\mathrm{D}}^{q}(r) = -\frac{Q}{4\pi\lambda_{\mathrm{D}}^{2}}\,\frac{e^{R_{\mathrm{eff}}/\lambda_{\mathrm{D}}}}{1+R_{\mathrm{eff}}/\lambda_{\mathrm{D}}}\,\frac{e^{-r/\lambda_{\mathrm{D}}}}{r},\ R>R_{\mathrm{eff}} \qquad \textbf{[S29]}$$

and $\rho_{\mathrm{D}}^{q}(r)=0$ otherwise, where R_{eff} is the effective radius of the colloid described in the main text, the Debye screening length is defined as

$$\lambda_{\mathrm{D}} = \sqrt{\frac{\epsilon}{\beta\left(\rho_{+}q_{+}^{2}+\rho_{-}q_{-}^{2}\right)}}, \qquad \textbf{[S30]}$$

and $\rho_{\pm}$ and $q_{\pm}$ are the density and charge of counter (+) or coions (−), respectively. Because we are concerned only with the long-ranged behavior of the solvent, we expect that a good description of the thermodynamics can be obtained by considering the asymptotic behavior $\rho_{\mathrm{D}}^{q}(r)$. Thus, we expand the Fourier transform of the Debye–Hückel charge density to second order as

$$\hat{\rho}_{\mathrm{D}}^{q}(k) \sim \hat{\rho}_{\mathrm{D}}^{(0)q} + k^{2}\hat{\rho}_{\mathrm{D}}^{(2)q}. \qquad \textbf{[S31]}$$

Here, the zeroth moment is given by

$$\hat{\rho}_{\mathrm{D}}^{(0)q} = 4\pi\int_{R_{\mathrm{eff}}}^{\infty} dr r^{2}\rho_{\mathrm{D}}^{q}(r) = -Q, \qquad \textbf{[S32]}$$

which is just a restatement of the electroneutrality of the system. Similarly, the second moment of the charge density is

$$\hat{\rho}_{\mathrm{D}}^{(2)q} = -\frac{4\pi}{6}\int_{R_{\mathrm{eff}}}^{\infty} dr r^{4}\rho_{\mathrm{D}}^{q}(r) = Q\lambda_{\mathrm{D}}^{2}C, \qquad \textbf{[S33]}$$

where

$$C \equiv \frac{\left[1+\left(\frac{R}{\lambda_{\mathrm{D}}}\right)+\frac{1}{2}\left(\frac{R}{\lambda_{\mathrm{D}}}\right)^{2}+\frac{1}{6}\left(\frac{R}{\lambda_{\mathrm{D}}}\right)^{3}\right]}{1+\left(\frac{R}{\lambda_{\mathrm{D}}}\right)}, \qquad \textbf{[S34]}$$

and the well-known form of the second moment relation is recovered when $R/\lambda_{\mathrm{D}} \ll 1$, such that $C \approx 1$. Note that for the case in the main text, $R = 30$ Å and $\lambda_{\mathrm{D}} = 26.8$ Å, such that R/λ_{D} is of order unity, and we therefore expect the following approximations for the free energy in terms of the moments of the charge density to only be of qualitative accuracy.

Using the approximation in Eq. **S31** for the charge density, the LMF free energy can be written as

$$\beta\Delta G_{\mathrm{LMF}} = -\frac{4\pi\beta Q^{2}}{2\epsilon(2\pi)^{3}}\int d\mathbf{k}\,\frac{e^{-k^{2}\sigma^{2}/4}}{k^{2}}\left[1-2k^{2}\lambda_{\mathrm{D}}^{2}C+k^{4}\lambda_{\mathrm{D}}^{4}C^{2}\right] \qquad \textbf{[S35]}$$

$$\equiv \beta\Delta G_{\mathrm{LMF}}^{(0)} + \beta\Delta G_{\mathrm{LMF}}^{(2)}, \qquad \textbf{[S36]}$$

such that $\Delta G_{\mathrm{LMF}}^{(0)}$ and $\Delta G_{\mathrm{LMF}}^{(2)}$ are the components of the free energy due to the zeroth and second moments of the charge density. The integrations can be readily performed, yielding

$$\beta\Delta G_{\mathrm{LMF}}^{(0)} = -\frac{\beta Q^{2}}{\epsilon\sigma\sqrt{\pi}}, \qquad \textbf{[S37]}$$

$$\beta\Delta G_{\mathrm{LMF}}^{(2)} = \frac{4\beta Q^{2}}{\epsilon\sigma\sqrt{\pi}}\left(\frac{\lambda_{\mathrm{D}}}{\sigma}\right)^{2}C - \frac{12\beta Q^{2}}{\epsilon\sigma\sqrt{\pi}}\left(\frac{\lambda_{\mathrm{D}}}{\sigma}\right)^{4}C^{2}, \qquad \textbf{[S38]}$$

such that the total LMF free energy is

$$\beta\Delta G_{\mathrm{LMF}} = -\frac{\beta Q^{2}}{\epsilon\sigma\sqrt{\pi}}\left[1-4\left(\frac{\lambda_{\mathrm{D}}}{\sigma}\right)^{2}C+12\left(\frac{\lambda_{\mathrm{D}}}{\sigma}\right)^{4}C^{2}\right]. \qquad \textbf{[S39]}$$

The contributions to ΔG_{LMF} are compared with simulation results in Fig. S3. Clearly, Eq. **S39** provides a qualitative description of ΔG_{LMF} that is improved by including higher moments of ρ_{D}^{q}; however, many higher-order terms in the moment expansion are needed to approach quantitative accuracy.

Ion Hydration

We now consider ion hydration as an example where the system has a net charge and long-ranged electrostatics play a significant role in solvation thermodynamics. Traditional approaches to ion solvation, such as the successful formalism developed by Hummer et al. (36), involve the simulation of a single ion in a dielectric solvent. The electrostatics are treated by Ewald summation in these systems and therefore require the presence of a neutralizing background charge density. In addition, significant finite size effects due to the periodicity of the Ewald sum are present (20), although successful finite-size corrections to the solvation free energy have been developed (21, 36, 47).

LMF theory provides a useful alternative to periodic lattice summation techniques when studying ion solvation. Aside from the efficient simulation of purely short-ranged systems afforded by LMF theory, the conceptual difficulties associated with a nonuniform effective electrostatic potential that depends on the size of the simulation cell can be eliminated. By using the iteration scheme in the following section, the LMF potential will display the asymptotic behavior predicted by classic electrostatics, $Q/\epsilon r$ for large r.

Following Hummer et al. (36), we consider the calculation of the solvation free energy of a charged methane-like particle in SPC water. In this case, methane is modeled in the united atom scheme, such that methane (Me) is represented as a single LJ particle with Me–water interaction parameters of $\varepsilon_{\mathrm{LJ}}^{\mathrm{Me-O}} = 0.893228$ kJ/mol and $\sigma_{\mathrm{LJ}}^{\mathrm{Me-O}} = 3.44778$ Å. We consider a cationic state of this particle, with charge $Q = +1$. Care is needed to ensure the proper asymptotic behavior of the system when solving the LMF equation for electrostatics, and we use the procedure described in the next section to solve the LMF equation for nonneutral systems.

We separate the solvation free energy $\check{G}$ of the positively charged methane ion following LMF theory:

$$\check{G} = \check{G}_{0} + \Delta G_{\mathrm{R1}} + \Delta G_{\mathrm{LMF}}. \qquad \textbf{[S40]}$$

The first term in Eq. **S40** is the solvation free energy of the ion in the SCA system. This can be divided into a free energy of inserting an uncharged cavity into the GT variant of SPC water, $\check{G}_{\mathrm{cav}}$, and a free energy of turning on the near-field portion of the ion charge, ΔG_{Q_0}, such that $\check{G}_{0} = \check{G}_{\mathrm{cav}} + \Delta G_{Q_0}$. The free energy of inserting the ion core can be readily determined by Widom particle insertion (3, 10), and here we used the value determined by Hummer et al. (36), $\check{G}_{\mathrm{cav}} = 10.2$ kJ/mol. This is equivalent to the value obtained for solvation in GT water to a good approximation, because the local structure and small-scale density fluctuations of the full water model are accurately described by the SC (GT) system (27, 28). The free energy of the near-field charging process was then determined by performing simulations of charged states $Q = 0$, 0.25, 0.5, 0.75, and 1.0 and calculating

the free energy as a function of Q using the Bennett acceptance ratio (39).

The hydration free energy of a methane-like cation in SPC water determined from LMF theory-based free energy calculations is compared with the results of ref. 36 in Table S1. The total solvation free energy $\check{G}$ listed there is corrected for finite system size by the addition of $\Delta G_{\mathrm{FS}} = Q^2\xi(1-1/\epsilon)/(2L)$, where $\xi = -2.38$ for a cubic simulation cell (36). The results obtained from the LMF theory compare well with the solvation free energies obtained in previous work (36). It is important to emphasize that the accurate LMF ion hydration free energies are obtained from relatively simple simulations of purely short-ranged systems and the many difficulties associated with traditional approaches to ion solvation using Ewald summation are avoided. The only essential correction to the free energy is simply to account for the finite size of the simulation cell.

Stable Iteration of the LMF Equation for Charged Systems

In this section we detail a stable iteration scheme for self-consistently solving the LMF equation when the system has a net charge. We consider here an ion with a point charge $Q\delta(\mathbf{r})$ fixed at the origin in SPC/E water. We accomplish this by introducing a second smoothing length, which additionally separates the long-ranged portion of the LMF potential into an intermediate and a final long-ranged component, whose limiting asymptotic form is known from classic electrostatics and can be approximated analytically. The intermediate ranged component of the potential is obtained self-consistently by a stable iteration method that ensures consistency with the known asymptotic form. In this section we will explicitly indicate the values of the Gaussian smoothing length for clarity.

We first separate the electrostatic LMF $\mathcal{V}_{\mathrm{R}}(\mathbf{r})$ in Eq. **8** in the main text into short- and long-ranged components (21) according to

$$\mathcal{V}_{\mathrm{R}}(\mathbf{r}) = \mathcal{V}_0(\mathbf{r}) + \mathcal{V}_{\mathrm{R1}}(\mathbf{r}), \qquad \textbf{[S41]}$$

where

$$\mathcal{V}_0(\mathbf{r}) = \int d\mathbf{r}' \rho^{Q}(\mathbf{r}') v_0(|\mathbf{r}-\mathbf{r}'|;\sigma) \qquad \textbf{[S42]}$$

is the short-ranged component of the ion potential and $\mathcal{V}_{\mathrm{R1}}(\mathbf{r})$ is the slowly varying portion of the total renormalized potential, given by

$$\begin{aligned}\mathcal{V}_{\mathrm{R1}}(\mathbf{r}) &= \int d\mathbf{r}' \left[\rho^{q}_{\mathrm{R}}(\mathbf{r}') + \rho^{Q}(\mathbf{r}')\right] v_1(|\mathbf{r}-\mathbf{r}'|;\sigma) \\ &= \int d\mathbf{r}' \rho^{q\sigma}_{\mathrm{R,tot}}(\mathbf{r}') \frac{1}{|\mathbf{r}-\mathbf{r}'|}.\end{aligned} \qquad \textbf{[S43]}$$

Here $\rho^{q}_{\mathrm{R}}(\mathbf{r})$ and $\rho^{q\sigma}_{\mathrm{R}}(\mathbf{r})$ are the bare and Gaussian smoothed charge densities of the mobile solvent, and $\rho^{Q}(\mathbf{r}) = Q\delta(\mathbf{r})$ and $\rho^{Q\sigma}(\mathbf{r}) = Q\rho_G(\mathbf{r};\sigma)$ are the bare and Gaussian smoothed charge densities of the ion, where $\rho_G(r;\sigma) = \sigma^{-3}\pi^{-3/2}\exp(-r^2/\sigma^2)$. Eq. **S43** shows that $\mathcal{V}_{\mathrm{R1}}(\mathbf{r})$ is the electrostatic potential arising from Gaussian smoothing of the total charge density $\rho^{q}_{\mathrm{R,tot}}(\mathbf{r}) = \rho^{q}_{\mathrm{R}}(\mathbf{r}) + \rho^{Q}(\mathbf{r})$.

Classic electrostatics tells us that the asymptotic form of the polarization potential

$$\Phi_{\mathrm{pol}}(\mathbf{r}) = \int d\mathbf{r}' \rho^{q}_{\mathrm{R,tot}}(\mathbf{r}') \frac{1}{|\mathbf{r}-\mathbf{r}'|} \qquad \textbf{[S44]}$$

induced by the ion is given by $Q/\epsilon r$ independent of the nature of the ion core, where ϵ is the known dielectric constant of the solvent (SPC/E water). We can generate this asymptotic form by approximating

$$\rho^{q}_{\mathrm{R,tot}}(\mathbf{r}') \sim \frac{Q}{\epsilon}\delta(\mathbf{r}') \qquad \textbf{[S45]}$$

in Eq. **S44**, consistent with the idea of water as a linear dielectric medium that screens all but a fraction Q/ϵ of the bare ion charge at large distances.

Eqs. **S41**–**S43** show that $\mathcal{V}_{\mathrm{R1}}(\mathbf{r})$ has exactly the same asymptotic form as $\Phi_{\mathrm{pol}}(\mathbf{r})$ and we will exploit this in the self-consistent solution of Eq. **S43**. To that end we treat $\mathcal{V}_{\mathrm{R1}}(\mathbf{r})$ as the total electrostatic potential in a new (σ-smoothed) system, and use LMF theory to map this system onto a new mimic system with an additional smoothing length l. This mapping separates $\mathcal{V}_{\mathrm{R1}}(\mathbf{r})$ into intermediate- and long-ranged components $\mathcal{V}_{\mathrm{R1}}(\mathbf{r}) = \mathcal{V}^{A}_{\mathrm{R1}}(\mathbf{r}) + \mathcal{V}^{B}_{\mathrm{R1}}(\mathbf{r})$. The long-ranged component $\mathcal{V}^{B}_{\mathrm{R1}}(\mathbf{r})$ is

$$\mathcal{V}^{B}_{\mathrm{R1}}(\mathbf{r}) = \int d\mathbf{r}' \rho^{q\sigma}_{\mathrm{R,tot}}(\mathbf{r}') v_1(|\mathbf{r}-\mathbf{r}'|;l) \qquad \textbf{[S46]}$$

$$= \int d\mathbf{r}' \rho^{q}_{\mathrm{R,tot}}(\mathbf{r}') v_1(|\mathbf{r}-\mathbf{r}'|;\sigma_l), \qquad \textbf{[S47]}$$

where

$$\sigma_l \equiv \sqrt{l^2+\sigma^2}. \qquad \textbf{[S48]}$$

To derive Eq. **S47** we combined the Gaussian convolutions in the definitions of $\rho^{q\sigma}_{\mathrm{R,tot}}$ and v_1 in Eq. **S46**.

We now choose l sufficiently large that we can use Eq. **S45** to accurately approximate the charge density in Eq. **S47**. This gives a simple analytic expression for the final long-ranged component

$$\mathcal{V}^{B}_{\mathrm{R1}}(\mathbf{r}) \approx \frac{Q}{\epsilon} v_1(\mathbf{r};\sigma_l), \qquad \textbf{[S49]}$$

such that $\mathcal{V}^{B}_{\mathrm{R1}}(\mathbf{r}) \to Q/\epsilon r$ as $r \to \infty$, which is the desired asymptotic behavior. In practice, we find that values of l on the order of σ suffice for this approximation to hold, and the results presented herein were obtained with $l = \sigma$.

This stable iteration scheme for systems with a net charge requires the self-consistent solution of the intermediate-ranged portion of the renormalized field

$$\mathcal{V}^{A}_{\mathrm{R1}}(\mathbf{r}) = \int d\mathbf{r}' \left[\rho^{q\sigma}_{\mathrm{R}}(\mathbf{r}') + Q\rho_G(\mathbf{r}';\sigma)\right] v_0(|\mathbf{r}-\mathbf{r}'|;l) \qquad \textbf{[S50]}$$

from simulation data; there are no numerical problems at large distances here because of the cutoff from $v_0(|\mathbf{r}-\mathbf{r}'|;l)$. The remaining long-ranged, slowly varying component $\mathcal{V}^{B}_{\mathrm{R1}}(\mathbf{r})$ is approximated by Eq. **S49** at each iteration.

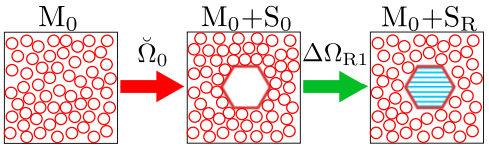

Fig. S1. Schematic illustration of the decomposition of the mimic system solvation free energy, $\breve{\Omega}_R$, into the solvation free energy of the SCA system, $\breve{\Omega}_0$, and the free energy of turning on the slowly varying portion of the LMF, $\Delta\Omega_{R1}$.

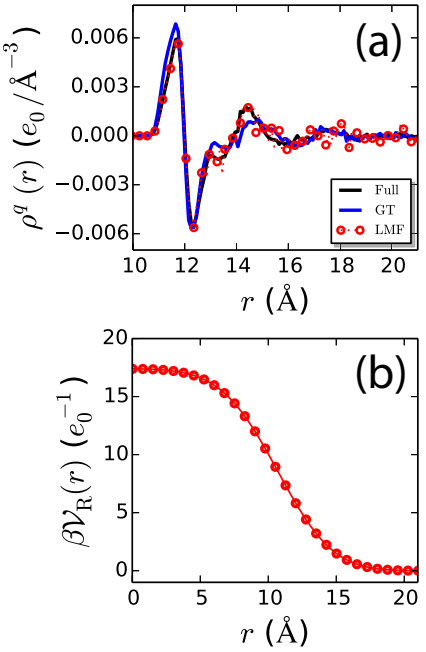

Fig. S2. (*A*) Charge density of water around a purely repulsive sphere with an effective hard sphere diameter of $R_{HS} = 12$ Å. The LMF charge density was determined using Eq. **S22**. (*B*) For completeness, we also show the electrostatic LMF $\mathcal{V}_R(r)$ that gives rise to the LMF charge density in *A*. Note that in this case the solute has no charge, $\mathcal{V}(\mathbf{r}) = 0$, such that $\mathcal{V}_R(r)$ arises solely from solvent–solvent interactions via renormalization.

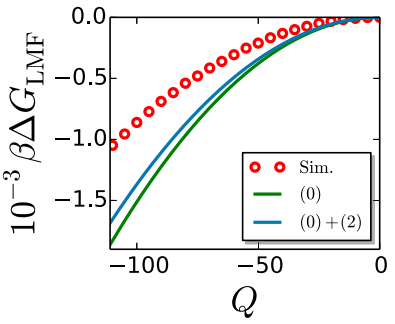

Fig. S3. LMF contribution to the colloid solvation free energy and two approximations to the free energy obtained from the first and second moments of the Debye charge density.

Table S1. Contributions to the ion solvation free energy (kJ/mol)

$\breve{G}_{Q_0}$	ΔG_{R1}	ΔG_{LMF}	$\breve{G}$	Hummer et al. (36)
−73	−63	−58	−244	−240